EVAPOTRANSPIRATON PARTITIONING USING STABLE WATER ISOTOPES IN A SEMI-ARID EVERGREEN FOREST

by

Jacob Meuth

A Thesis Submitted to the Faculty of the

DEPARTMENT OF ATMOSPHERIC SCIENCE

In Partial Fulfillment of the Requirements

For the Degree of

MASTER OF SCIENCE

WITH A MAJOR IN HYDROMETEOROLOGY

In the Graduate College

THE UNIVERSITY OF ARIZONA

2012

STATEMENT BY AUTHOR

This thesis has been submitted in partial fulfillment of the requirements for an advanced degree at The University of Arizona and is deposited in the University Library to be made available to borrowers under rules of the Library.

Brief quotations from this thesis are allowable without special permission, provided that accurate acknowledgment of source is made. Request for permission for extended quotation from or reproduction of this manuscript in whole or in part may be granted by the head of the major department or the Dean of the Graduate College when in his or her judgment the proposed use of the material is in the interests of the scholarship. In all other instances, however, permission must be obtained from the author.

Signed: Jacob Meuth

APPROVAL BY THESIS DIRECTOR

This thesis has been approved on the date shown below:

Francina Dominguez
Assistant Professor of Atmospheric Science

April 17, 2012
Date

TABLE OF CONTENTS

TALBE OF CONTENTS - Continued

ABSTRACT

Total evapotranspiration (ET) is the key process that links the land and the atmosphere via water, energy and carbon exchange. ET is a combination of evaporation and transpiration, which behave dynamically in very different ways. In this work we investigate the relative contribution of transpiration and soil evaporation to total ET in a semi-wooded, semi-arid forest in the Manitou Research Park northwest of Colorado Springs, CO. We use stable water isotopes measured at different levels within and outside the canopy, over a 30-day period (June 26 - July 26, 2010), using a field-deployable cavity ring-down spectrometer. The traditional "Keeling plot" analysis is used to partition the ET flux from moisture that comes from outside of the ecosystem, and then a simple model is used to partition the transpiration flux. In addition, we introduce a new alternative "multi-level" method to calculate the fraction of transpiration to total ET. Both the "Keeling plot" method and the "multi-level" method yield very similar fractions of transpiration to total ET, ranging from about 15% to about 85%. We compare both methodologies and discuss some of the corrections that must be made when measuring with high-frequency field-deployable instruments.

1. INTRODUCTION

Our understanding of hydrometeorological processes relies primarily on observations from different sources; radiosondes, meteorological stations, flux towers and measurements at the surface and subsurface. When translating our knowledge into numerical models, variables that cannot be measured must be parameterized in order for the model to make the best estimations. Two of these variables are evaporation (E) and transpiration (T) fluxes over land. Total evapotranspiration (ET) is the key process that links the land and the atmosphere via water, energy and carbon exchange. ET is a combination of E and T that behave dynamically in very different ways. E is often a faster process related primarily to surface and shallow subsurface water storage while T is usually a slower process that links deeper sources of moisture to the atmosphere and hence imparts longer-term memory to the atmosphere-terrestrial system (Scott and Koster, 1997). Even if ET is adequately represented in land surface models, the temporal dynamics will not be correct if the relative contribution of E and T to ET is not realistically described (Scott et al., 1995). An accurate representation of E/T partitioning is particularly important in climate models. If E accounts for a large fraction of ET, the timescale of response of the land-atmosphere system is shortened and the land is less likely to influence model persistence, shortening the memory in the system and likely affecting downstream regions (Scott et al.,

1997). In addition, terrestrial ET fluxes make up a large portion of precipitation in many parts of the world (Salati and Vose, 1984; Van der Ent et al. 2010). Numerous modeling methods have been used to track precipitation originating as ET, including back trajectory algorithms (Dirmeyer and Brubaker, 1999), analytical models, (Brubaker et al. 1993, Dominguez et al. 2006) or numerical water vapor tracers (Bosilovich and Schubert, 2002; Bosilovich and Chern, 2006). Many of these models rely on the ET flux as part of their algorithm (Dirmeyer and Brubaker, 1999; Dominguez, 2006). These data sets tend to come from other models such as the National Center for Enviromental Prediction (NCEP) reanalysis model (Kalnay et al. 1996) or North American Regional Reanalysis (NARR) data (Mesinger et al. 2006) (Dirmeyer and Brubaker, 1999; Dominguez et al., 2008). However, NCEP reanalysis ET is known to be uncertain (Betts et al. 1996), and the more recent NARR dataset does not include a direct correction of ET flux and is therefore subject to error (Nigam and Ruiz-Barradas, 2006). Modeling approaches have also been used to assign probabilistic estimates of T and E in semiarid ecosystems (Paruelo and Sala, 1995; Reynolds et al. 2000). But as with all modeling approaches, field studies are needed to verify and increase the accuracy and reliability of the models.

In order to close the water balance, ET values must be estimated with a greater degree of accuracy (Fisher et al. 2008). In addition, ET must be

separated into its individual components for it to be useful in modeling ecosystem change. Land surface models rely on land cover and land use information; when the ecosystem changes, the model must use new land surface parameters (such as stomatal conductance or albedo) for estimating ET flux. There are several methods to measure ET as a whole or its individual components (Wilson et al., 2001, Kostner,2000., Sala et al.,2000). The use of micrometeorological methods such as eddy covariance (EC) or Bowen ratio have been routinely used to measure total ET (Shuttleworth et al., 1988; Moncrieff et al., 2000; Baldocchi et al., 1988). These methods account for the total ET flux, but do not give any indication of the contribution from different components of the ecosystem. Plant transpiration can be measured using chamber gas exchange and sap flow methods, which account for the function of physiological and environmental controls (Pearcy et al., 1988; Jackson et al., 2000). However, poor spatial representation continues to be the Achilles heel in their application at ecosystem or larger spatial scales as individual trees must be measured (Jarvis, 1995; Ehleringer and Field, 1993). Soil weighing lisymeters and soil water budgets are used to measure soil evaporation, but these measurements are difficult and expensive to implement, and often have poor spatial representation (Dunin, 1991).

The use of stable isotope methods offers great promise for partitioning flux at the ecosystem scale as they are easily measured and can be used in many environments, just like the methods listed above (Brunel et al., 1992, Moreira et al., 1997, Yakir and Wang, 1996, Wang and Yakir, 2000; Yepez, 2003). Using stable isotopes entails measuring the ratio of heavier to lighter isotopes of both hydrogen and oxygen molecules of water namely ^{18}O and $^{2}H(D)$ (Clark Fritz, 1997). When transpiration is at isotopic steady state, the isotopic composition of the transpired vapor equals that of the water up taken by the plants, since no fractionation will occur from root uptake to transpiration at the leaf surface (Flanagan et al., 1991). Soil vapor however, is greatly fractionated during evaporation causing the vapor to be greatly depleted (Craig and Gordon, 1965; Gat, 1996). Consequently, there is often a significant difference between the isotopic composition of the highly fractionated evaporation flux from the soil and the non-fractionated transpiration flux from the plants. These differences, and their interaction with the vapor in the ecosystem boundary layer, is the basis for partitioning fluxes using isotopic analysis, since the isotopic composition of a vapor sample reflects the mixture of the contributing sources and the background air (Yakir and Wang, 1996). A method known as the 'Keeling plot analysis' allows for the determination of the isotopic composition of ET from the mixing of plant transpiration and soil evaporation in the study area by

eliminating the outside sources (Keeling, 1958,1961, Moreira, 1997, Williams et al., 2004). From the determination of the steady state components of transpiration and soil evaporation (the end members), it is possible to separate the contribution of transpiration and soil evaporation from the total ecosystem vapor. This method relies on the assumption of steady state of the isotopic composition of leaf transpiration as measured by the isotopic composition of stem water (Wang and Yakir,2000). This method also relies on the assumption that the soil is in isotopic equilibrium and that the evaporation from the soil can be calculated using conditions that can be measured, for example: humidity, temperature, and initial soil water isotopic composition, and the equations derived by Craig and Gordon (1965) (Moriera et al. 1997; Wang and Yakir, 2000; Yepez et al., 2003, 2005).

In the past, the most common way to sample isotopes from the air was to use cryogenic trapping. Cryogenic trapping pulls air through a tube and into traps that are submerged in some sort of medium that is well below freezing, to condense and freeze water vapor to the traps. This process is time consuming and limited by the number of samples taken per time period. However, new instruments that can take high-frequency measurements of isotopic composition are available. Two isotopic measurement instruments are field deployable and transportable with relative ease; one manufactured by Picarro and another by Los Gatos. They both us laser technology to

analyze the water vapor that passes through the cavity inside the instrument. The Picarro cavity ring-down spectrometer is a desktop computer sized analyzer with an auto sampler that allows for calibration of the unit in the field. Los Gatos also makes a field type analyzer, this instrument has higher accuracy than the Picarro instrument but is much less transportable and has a limited range of temperatures that it can be deployed in. Both of these instruments can perform measurements continuously. A Picarro cavity ring down spectrometer was used for all measurements in this study, a detailed description of the instrument will follow.

The goals of this paper are:

1) To quantify the relative contribution of T and E to total ET flux in a semi arid sparse forest in Colorado for the months of June and July of 2010 using a Picarro isotopic analyzer.
2) Present the benefits of using rapid measurements, as well as some of the problems with using isotopic measurements for E and T partitioning.
3) Present a new method for partitioning the T and E flux. This new method will be compared against the Keeling plot isotopic method for further validation.

2. THEORETICAL OVERVIEW

2.1. Fractionation of Water

Water molecules have two distinct stable isotopes, O (18, 16) and H (2, 1). Fractionation is the process of changing ratios of heavy to light isotopes, either through evaporation or condensation (Clark Fritz, 1997). Using the differences in mass of the molecules, we can track the source of water in its different phases through the different fractionation rates that occur as a result of evaporation or transpiration at the leaf stomata. The standard for denoting isotopic signature is delta notation (δ) in per mil (‰) (Ehleringer et al., 2000).

$$\delta = \frac{R_{sample} - R_{standard}}{R_{standard}} * 1000 \quad (1)$$

where R is the molar ratio of the heavy to light isotopes in the sample and the appropriate standard. Lower delta values denote higher fractionation factor compared to the standard, or that the water has less ^{18}O molecules per million molecules sampled. The samples are tested against a standard in order to have a way of comparing them to each other.

2.2. Leaf Water Fractionation

The isotopic composition of water transpiring from leaves has traditionally be characterized either in steady state, or by taking into account the intra-diurnal variability of isotopic composition of the leaves. There is no isotopic fractionation of water by uptake of plants and its transport to leaf stomata (Ehleringer and Dawson, 1992; Brunel et al., 1995). However, isotopic enrichment may occur during transpiration as a result of kinetic and equilibrium fractionation factors (Flannigan and Ehleringer, 1991; Flannigan et al., 1991). During the diurnal cycle of transpiration an isotopic steady state can be achieved, in this state the isotopic composition of transpiration out of the leaf is equivalent to that of the moisture source at root uptake. This steady state requires an interval of time after conditions outside the leaf change (Wang and Yakir, 1995). Changes can be: increased sunlight resulting in increased photosynthesis or changes in atmospheric moisture content. This allows for us to be able to assume stem water is equivalent to isotopically to transpiration although fractionation is occurring at the stomata opening. Over short-term periods (hourly) water vapor exiting the leaf stomata can be different than that coming to the leaf from the stem (Wang and Yakir, 1995). The magnitude of this change in isotopic composition is dependent on species and the amount of change in relative humidity, as well as leaf water turnover time (Wang and Yakir, 1995). For

the purposes of this study we are interested in steady state only. The following derivation is for leaves in steady state with the environment.

Equilibrium fractionation is defined as:

$$\dot{\alpha}^* = R_l / R_v \quad (2)$$

where R is the molar ratio of the heavy to the light isotope and the subscripts l and v refer to liquid or water vapor respectively (Craig and Gordon, 1965). It is assumed that the temperature of both liquid and vapor are the same. For a leaf, these conditions are satisfied when water in the intercellular air spaces and leaf cell water are in equilibrium (Flanagan et al, 1991). Since temperature plays a role in equilibrium fractionation, a series of measurements were performed by Majoube (1971) and regression equations were found in order to calculate $\dot{\alpha}^*$:

$$10^3 ln\dot{\alpha}^* = a\left(\frac{10^6}{T_K^2}\right) + b\left(\frac{10^3}{T_K}\right) + c \quad (3)$$

where T_K is temperature in Kelvin and a, b and c are constants described in Majoube (1971).

Kinetic fractionation is the ratio of the diffusion coefficients containing heavy and light isotopes. It is defined by:

$$\dot{\alpha}_k = g/g' \quad (4)$$

where g and g' refer to the stomatal conductance of water vapor molecules containing the light and heavy isotopes respectively. The values of $\dot{\alpha}_k$ are $^{16}O/^{18}O = 1.0285$ and for H/D are 1.025 (Merlivat, 1978). The values have to be modified to account for boundary layer turbulence outside the stomata pore. The values are modified by raising them to the two-thirds power (Kays, 1980). Thus, the final values for $\dot{\alpha}_k$ are $^{16}O/^{18}O = 1.0189$ and H/D = 1.017 (Flanagan, 1991).

Leaf water isotopic composition is important to finding the total amount of transpired water vapor. During steady state, the isotopic composition can be calculated from the isotopic composition of the water still in the leaf. This can be used as a check to the stem water transpiration assumption. The following derivation is a proof to show mathematically that stem water has the same composition as the transpired water vapor. To obtain an equation for isotopic leaf composition described in (Flanagan, 1991), we must first start with the transpiration rate of a leaf E which is described as:

$$E = g\left[\frac{e_i - e_a}{P}\right] \quad (5)$$

where e_i and e_a are the partial pressures of water vapor in the leaf intercellular air spaces and P the atmospheric pressure, respectively. A similar equation can be written for the heavy isotope molecules:

$$E' = \frac{g'\{R_i e_i - R_a e_a)}{P} \quad (6)$$

where e_i is multiplied by R_i the molar ratio of the heavy and light isotopes of water vapor in the intercellular spaces, and e_a is multiplied by R_a the molar ration of the heavy and light isotopes outside the leaf.

R_l is the isotopic compostion of the leaf water. The molar ratio of heavy to light isotopes in the transpiration stream (E'/E") can be approximated by the molar ratio of heavy isotopes to total water vapor transpired (E'/E) to simplify the following derivation. Inserting the above fractionation factors, the equation for the isotopic ratio of the transpired water becomes:

$$\frac{E'}{E"} = R_l \approx \frac{E}{E'} = \frac{1}{\dot{\alpha}_k} \frac{\left(\frac{R_l}{\dot{\alpha}*} e_i - R_a e_a\right)}{(e_i - e_a)} \quad (7)$$

At steady state, the isotopic composition of transpired water must be the same as the source or stem water. Therefore R_x, the isotopic composition of the source water, is defined as:

$$R_x = \frac{1}{\dot{a}_k}\frac{\left(\frac{R_l}{\dot{a}*}e_i - R_a e_a\right)}{(e_i - e_a)} \quad (8)$$

Rearranging to solve for R_l

$$R_l = \dot{a}^*[\dot{a}_k R_x\left(\frac{e_i - e_a}{e_i}\right) + R_a(\frac{e_a}{e_i})\,] \quad (9)$$

Equation 8 assumes that there are no significant boundary layer effects and therefore the partial pressure of water vapor at the lead surface (e_s) is the same as e_a. Equations 10and 11below take into account boundary layer effects. These two equations represent transport thought the stomata and the boundary layer separately.

$$R_x = \frac{1}{\dot{a}_k}\frac{\left(\frac{R_l}{\dot{a}*}e_i - R_s e_s\right)}{(e_i - e_s)} \quad (10)$$

$$R_x = \frac{1}{\dot{a}_{kb}}\frac{(R_s e_s - R_a e_a)}{(e_i - e_a)} \quad (11)$$

R_s is the molar ratio of the heavy and light isotopes of water vapor in the air at the leaf surface and $\dot{\alpha}_{kb}$ is the ratio of the conductance of the light and heavy isotopes in the boundary layer.

To obtain the equation for isotopic composition of leaf water, equation (10) is solved for R_s and then the resulting expression is inserted into equation (9) this will allow us to calculate the leaf water composition from known values, when the leaf is in steady state. The following equation can be used to calculate transpiration for water extracted from the leaf.

$$R_l = \dot{\alpha}^* [\dot{\alpha}_k R_x \left(\frac{e_i - e_a}{e_i}\right) + \dot{\alpha}_{kb} R_x \left(\frac{e_s - e_a}{e_i}\right) + R_a (\frac{e_a}{e_i}) \quad (12)$$

It is important to note, however, that for this study we used stem water, as opposed to leaf water, to estimate the isotopic composition of transpiration. Consequently, we are assuming that the system is at steady state. However leaf samples were taken in addition to stem samples as a backup in case the stem samples proved to be inadequate.

2.3. Isotopic Fractionation of Soil Moisture

When water evaporates from the soil, heavy isotopes are left behind depleting the evaporated water vapor. Temperature, relative humidity and atmospheric isotopic composition play a role in this depletion function as well

as equilibrium and kinetic fractionation factors (Craig and Gordon, 1965 and Gat, 1996). Fractionation in the soil is explained in Moreira (1997). We can use the same equations we used for leaf water transpiration as the basis for soil water fractionation. Starting with equations 2 and 3 we can derive equation 10. To describe soil water fractionation as a form in which all that is needed is relative humidity, Moreira (1997) made the assumption that the temperature above the surface and at the soil surface at the evaporation plane are the same. Then equation 11 becomes:

$$R_e = \left(\frac{1}{\dot{\alpha}_k}\right)\left[\frac{\frac{R_S}{\dot{\alpha}^*} - R_S H}{1-H}\right] \tag{13}$$

where H is relative humidity of the air and R_e is the isotopic composition of the evaporated soil water.

2.4. Flux Partitioning

Flux partitioning in an ecosystem is possible if the background isotopic signature is known, as well as the isotopic signature of total ET from the ecosystem. To find the ET signature, a Keeling plot analysis can be used (Keeling 1961). This is a mass balance mixing relationship that uses samples of air at different heights above the ground plotted against the inverse of the concentration of the substance of interest (Flanagan and

Ehleringer, 1998; Yakir and da Sternberg, 2000; Moreira, 1997; Yepez et al, 2003). The relationship is linear and when used with water vapor, the y-intercept shows the isotopic signature of the evapotranspiration flux:

$$\delta_{ebl} = C_a(\delta_a - \delta_{ET})\left(\frac{1}{C_{ebl}}\right) + \delta_{ET} \quad (14)$$

Where δ_{ebl} is the isotopic composition of vapor collected from the ecosystem boundary layer, C_a the atmospheric vapor composition, C_{ebl} the vapor concentration(humidity) in the ecosystem boundary layer, δ_a is the isotopic composition of the atmospheric background and δ_{ET} indicates the isotopic composition of the evapotranspiration flux. Standard error of these can be calculated based on the uncertainty produced by the variability of the sources and the regression coefficient of the Keeling Plots (Phillips and Gregg, 2001). The fractional contribution of transpiration to the evapotranspiration flux is then defined by:

$$F_T(\%) = \frac{\delta_{ET} - \delta_E}{\delta_T - \delta_E} * 100 \quad (15)$$

where δ_{ET} is the isotopic composition of evapotranspiration vapor, δ_E is the isotopic composition of vapor from soil sources (Eq 13) and δ_T is the isotopic composition of the transpiration vapor sources (Yakir and da Sternberg,

2000). Both δ_E and δ_T are calculated in advance using the methodologies described above.

2.4.1. **Assumptions of the Keeling plots**

This Keeling plot approach is limited by the assumption that the atmospheric concentration of vapor in the ecosystem is from only two major sources: the background atmospheric source and the sources of evapotranspiration added by the ecosystem (Yepez et al. 2003). It is also assumed that the losses of water vapor from the system are by turbulent mixing only, and not from condensation (Yepez et al. 2003). Furthermore, the gradient in water vapor concentration and isotopic composition must be large enough for a statistically significant regression line to be generated (Wang and Yakir, 2003). This last constraint implies that the Keeling plots are not useful during periods of intense mixing, when the water vapor and the isotopic composition of the water vapor in the ecosystem boundary layer has virtually no vertical gradient.

2.4.2. **Statistical Analysis of Keeling plots**

The Keeling plot analysis has limitations. The Keeling plot is a simple linear regression of the inverse of the specific humidity plotted under the delta values of the air samples. To find the isotopic composition of ET using the Keeling plot analysis, we find the regression equation and the confidence

intervals at the 95 percent level. These statistics were compared to the soil and stem data to determine if the Keeling plots fell within the end points of the data.

The equations used to find the fitted regression are as follows. All equations for the statistical analysis were taken from the Weibull DOE webpage for linear regression (www.weibull.com).

$$\hat{\beta}_1 = \frac{\sum_{i-1}^{n} y_i x_i - \frac{\left(\sum_{i-1}^{n} y_i\right)\left(\sum_{i-1}^{n} x_i\right)}{n}}{\sum_{i-1}^{n} (x_i - \bar{x})^2} \tag{16}$$

$$\hat{\beta}_0 = \bar{y} - \hat{\beta}_1 \bar{x} \tag{17}$$

$$\hat{y} = \hat{\beta}_0 + \hat{\beta}_1 x \tag{18}$$

where X_i is the inverse of the specific humidity Y_i is the delta value of the air sample, $\bar{y}$ is the average of data points in Y_i and Xbar is the average of all points for the inverse of specific humidity. β_1 is the regression coefficient. β_0 is the y intercept which is the critical number we are looking for, and indicates the isotopic composition of ET.Y is the predictor, the inverse of

specific humidity, and X is the predictand, the delta value of the air sample. This gives us the equation of the best-fit line to the dataset.

To find the explained variance of the regression line we use the following equations; where 19 is the variance of the residuals and 20 is the total variance:

$$SS_R = \sum_{i=1}^{n} (\hat{y}_i - \bar{y})^2 \tag{19}$$

$$SS_T = \sum_{i=1}^{n} (y_i - \bar{y})^2 \tag{20}$$

To find the R^2 or explained variance in a percent we take:

$$R^2 = 1 - \frac{SSr}{SSt} \tag{21}$$

To find the confidence interval on Beta0, we use the following equations:

$$e_i = y_i - \hat{y}_i \tag{22}$$

$$se(\hat{\beta}_0) = \sqrt{\frac{\sum_{i-1}^{n} e_i^2}{n-2}\left[\frac{1}{n} + \frac{\bar{x}^2}{\sum_{i-1}^{n}(x_i - \bar{x})^2}\right]} \tag{23}$$

$$\hat{\beta}_0 \pm t_{\alpha/2,n-2} \cdot se(\hat{\beta}_0) \tag{24}$$

where *se* is the standard error for β_0 and t_α is the t statistic from the student's t-table. This will give us the values above or below our y-intercept.

2.5. Multi-level Analysis

In addition to the Keeling plot analysis, we introduce a new analysis method to perform the transpiration calculations. This method involves using the absolute humidity and isotopic composition at each level averaged over a significantly long period in order to account for fluxes in the canopy. We assume that the top level was always drier than the bottom levels and that the humidity at the top level represented the background water vapor and did not change throughout the profile. Figure 1 shows a diagram of the theory behind the multi-level method.

The isotopic content at the *i* th level is given by:

$$\delta_i q_i = \delta_a q_a + \delta_T (q_{iT} - q_a) + \delta_S (q_i - q_{iT}) \quad (25)$$

where δ_i is the isotopic composition at the *i*th level q_i is the absolute humidity at the same level,δ_a is the isotopic composition at the top level q_{a+} is absolute humidity at the top level, q_{iT} is the absolute humidity of plant transpiration, δ_S is the isotopic composition of the soil evaporation and q_i is the absolute humidity at the *i*th level.

Rearranging equation (25) gives us equation (26) and furthermore solving for q_{iT} yields equation (27) which gives us the absolute humidity value for plant transpiration

$$\delta_i q_i = \delta_a q_a + \delta_T q_{iT} - \delta_T q_a + \delta_S q_i - \delta_S q_{iT} \quad (26)$$

$$\therefore \quad q_{iT}(\delta_T - \delta_S) = \delta_i q_i - \delta_S q_i + \delta_T q_a - \delta_a q_a$$

$$\therefore \quad q_{iT} = \frac{q_i(\delta_i - \delta_S) + q_a(\delta_T - \delta_a)}{(\delta_T - \delta_S)} \quad (27)$$

Assuming the humidity and isotopic content at the highest level (Level 1) is a reasonable approximation to those in the overlying atmosphere, and that the 5 lower levels at which measurements are made adequately sample the profiles of humidity and isotopic content in the canopy, then the total transpiration flux is given as a fraction of the total evaporation flux by:

$$F_T = \frac{\sum_{2}^{6}(q_{iT} - q_1)}{\sum_{2}^{6}(q_i - q_1)} \tag{28}$$

where F_t is the transpiration percentage, and q_1 is the absolute humidity at the top level. As stated above, the main assumption with this method is that the humidity at the top level (Level 1) and the isotopic concentration at this level are representing only the background atmosphere. This implies that T and E do not contribute to humidity at this level.

2.6. Drift Correction

We made a correction for time drift due to the fact that the Keeling plot relies on a linear regression based on simultaneous measurements taken throughout the canopy. The need for this correction was evident after processing the raw data, as it became apparent that large-scale meteorological processes outside the ecosystem primarily drove the variability of isotopic concentrations. To correct for this, a weighted average was calculated to correct for the change in moisture and composition with time. The top (Level 1) was taken as the starting point and levels 2 through 6 were averaged using a weighting factor in the following:

$$\delta = \frac{\delta_1 x + \delta_2 y}{2} \tag{29}$$

where δ is the new value for the time period(for q,δD,$\delta^{18}O$), δ_1 is the value before the current time and δ_2 is the value in the time after the current time and x and y are the weighting factors that change with each level. Figure 2 illustrates what the data would truly look like, shown in black dots. The open circles shows what the keeling plot relies upon and what the new drift corrected data would look like using equation 29.

3. METHODS

3.1. Site and measurement period

The study site is located in the Manitou Experimental Forest, 48 kilometers northwest of Colorado Springs, CO. The location is a 6,758 ha forest with limited human impacts in the area. It consists of dry-site Ponderosa Pine(*Pinus ponderosa*) and Douglas Fir (*Pseudotsuga menziesii)* forests intermixed with grassland parks and Aspen Clones(*Populus tremuloides).* The climate in this region has a wide range of temperatures with the summer temperatures reaching highs in the low 30^{o} C's and the lows in the winter reaching into the -20^{o}s C's. The seasonal average rainfall for the past 65 years is 395 ml/year (U.S. Department of Agriculture (USDA) website). The soils in the area are derived from the weakly structured Pikes Peak granite and are highly erodible with most being poorly developed with little organic matter except those in riparian areas (USDA). The location was chosen because measurements of one chemical tower and one meteorological tower, located a few meters apart are available as to complement our measurements. These two towers, as well as the suite of additional instruments, are part of several ongoing projects through the National Center for Atmospheric Research (NCAR). One of the towers (located at 7500' elevation, lat. 39°6'0" N, long. 105°5'30" W) includes chemical analysis tubing at 6 different levels that was easily adapted to the Picarro instrument.

Isotopic measurements were taken continuously from June 24th to July 27th, 2010. This compliments the center main growing season in Colorado. However, we will focus our attention on three days within this period: June 30th, July 9th and July 16th. Only during these days were we able to obtain the vegetation and soil samples required for ET partitioning.

3.1.1. **Meteorological Conditions**

During the 30-day period of measurement, the weather conditions were around the 30 year climate mean; no records were set. Significant precipitation events (Figure 3) were present leading up to the 30th of June with 0.77 cm of precipitation on June 27th. No precipitation fell on the 28th, 29th, or the 30th. Leading up to the 9th of July, there were three precipitation events that occurred. On the 7th, in the early afternoon a storm produced 1.6 cm of precipitation in a 20-minute period. In the evening of the 7th, another storm produced 0.62 cm of precipitation and a third precipitation event on the 8th produced 0.66 cm of rainfall in the early afternoon starting around 11:45pm and ending around 1:55pm. Wind conditions throughout the night were in the 0.3ms^{-1} to 0.8ms^{-1} range leading up into the morning of the 9th. During the 9th a 0.45 cm precipitation event occurred at beginning 12:45am. On July 14th,0.046 cm of precipitation fell in a 5 min period at 9:55pm,no precipitation was recorded on the 15th, wind conditions were in the 0.3ms^{-1} to 1.3 ms^{-1} leading up to the morning of the 16th, where no

precipitation occurred.

Throughout the days, sensible and latent heat were calculated as a way to find out where energy uptake by the atmospheric boundary layer was occurring (Figure 4). During the 30th of June and the 16th of July we find that most radiation is being converted into sensible heat while much less is being converted into evaporative processes. During the morning of the 16th, there was a spike in latent heat flux this is most likely due to dew being evaporated. On the 9th of July we find, due to the prior two days rainfall events, that about half of the solar radiation is being converted to sensible heat, while the other half is being used for evaporative processes. We can see the effect that a wet soil medium (Figure 4 middle) has on the latent and sensible heat parameters by increasing latent heat and decreasing sensible heat throughout the day.

Wind speed was monitored at 4 different levels throughout the canopy, 1.7, 7, 14, and 27 meters (figure 4). We can see that for most of the daily time periods we have wind speeds above 2 ms^{-1}at the 27 meter level. Lower levels had lower wind speeds with the lowest level tending to have wind speeds in the 0.3 to 1.5 ms^{-1} range throughout the three days. We found that the 7 meter level had the lowest wind speeds for all three days. This would tend to lead to mixing of the upper air down into the middle levels due to turbulence.

3.2. Data Collection

3.2.1. Vapor Data

We used a Picarro cavity ring down spectrometer for the collection and processing of water vapor and isotopic composition of water vapor in the air. We collected water vapor at six different levels in order to make Keeling plots with a high statistical accuracy. Vapor was collected via Teflon tubing from 25.3, 17.7, 12 8.5, 5 and 1.6 meter heights. We collected water vapor through each line into a 6 port vacuum manifold with continuous flow. A secondary set of solenoid switches controlled the valves to allow 5 minutes of airflow per level, and the Picarro provided isotopic measurements at 5-second intervals. The process of measuring the 6 levels took 30 minutes and then would repeat 48 times a day. The data was then averaged over each time period (5-minutes for every level) and we plotted each level versus the inverse of specific humidity at each different level to construct the Keeling plots.

3.2.2. Stem and Soil Data

In order to procure the liquid water from the soils and the stems, we collected samples at specific times from numerous trees. Stem samples from 3 different ponderosa pine trees were taken at 1:30 pm on the 30th of June and the 9th and 16th of July. Soil samples were collected at the 1:00 pm and were taken at 5, 10, 20, 30, 40, and 50 cm depths. These samples were taken in glass vials with screw top lids, then wrapped with paraffin film and then

frozen to keep any water vapor from escaping the vial. We used a cryogenic extraction line to extract the water from the stem and soil samples. After the water was extracted at the NCAR foothills lab, the Picarro instrument was used to analyze the isotopic composition of the water.

3.3. Picarro Cavity Ring Down Spectrometer

A Picarro cavity ring down spectrometer model L2120-i was used to analyze all the data vapor and liquid samples. The machine uses, time based cavity ring-down spectrometry with a laser to quantify spectral features of gas phase molecules. The machine has a precision of 0.5‰ for δD and 0.1‰ for $\delta^{18}O$ for liquid injected samples and a 1.0‰ for δD and 0.2‰ for $\delta^{18}O$ precision for water vapor sampling. (Specifications were taken from the Picarro data sheet on from the Picarro webpage www.picarro.com) In order to perform the analysis on the liquid samples, they were transferred to small vials and injected by the machine into the instrument's vaporizer. After the sample has been vaporized, it is sent by way of a 4 inch heated copper tube into the cavity of the spectrometer. A laser passes though the sample various times reflecting off a series of mirrors which give the laser an effective path length of 12 km, this insures a high quality measurement of isotopic composition and specific humidity. The measurement process takes approximately 3 minutes and the sample is ejected through a port out of the machine. Ultra high purity nitrogen is then flooded into the cavity and

vaporizer chamber to insure that no moisture from the previous sample remains.

4. MACHINE ANALYSIS

4.1. Analysis of Picarro instrument against NCAR's LiCor data and other instrumental fixes.

The Picarro instrument was set up alongside a LiCor Li6262 that NCAR has been monitoring absolute humidity with for a number of years. We validated the Picarro measurements of absolute humidity against those of the NCAR instrument. We found that the Picarro has a positive bias in the measurement of absolute humidity with respect to the NCAR instrument over the periods in which we are interested (Figure 7). This could have an effect on the Keeling plots, as the inverse of absolute humidity is used, and a positive bias could cause shifts in the Keeling plots. By changing the specific humidity values the line can be shifted to the left or right as well as changing the slope. However it will not cause any bias in the multi-level method as that method calculates the percentage of T to ET. We looked into fixing the issue between the two instruments assuming that the NCAR values were closer to being correct. However, since the Picarro relies on absolute humidity to make isotopic composition measurements, the humidity and isotopic composition are related and we cannot substitute the NCAR measurements for the Picarro. In Figure 6, a simple subtraction 2.2gm/kg, the average daily difference, was made from the Picarro specific humidity. This results in a slope change and a y-intercept slightly lower than the raw

data. However, we found that the error was small enough to have little effect on the Keeling plots (Figure 6) and have assumed that the Picarro specific humidity is correct.

All Keeling plots and multi-level analysis were performed using the raw Picarro dataset. Unfortunately, with the instruments there were some technical difficulties; on June 30th the NCAR machine did not record any data and thus we cannot compare it to the Picarro data; on July 9th the NCAR machine only recorded data after the rainfall event (12:00pm) which made it impossible to compare during the period in which the Keeling plots were produced. On July 16th the Picarro had a malfunction in the morning.

4.1.1. **Changes in the tubes**

We must account for any mixing in the tube before the air arrived to the Picarro when the solenoid valve switched to receive air from different sources. As the Picarro draws in a relatively small amount of air with each sample (~40sccm @ 760 torr) there is potential mixing in the tube with air from different levels. After carefully analyzing the data, it appears that the first minute and a half was mixed air and then the measurements seemed to be more even until the next change in level (Figure 8). We also noticed that mixing did not seem to be the only problem as we would get an uptick in the data every time the solenoid changed this cannot be mixing, as it occurred in the fix two minutes it was discarded. While we believe all the mixed air was

replaced with air from a single level after a minute and a half, we disregarded the first two minutes, and took the final 3 minutes worth of data per level to be sure no mixing was occurring.

5. RESULTS

5.1.Analyzed Samples

5.1.1. Soil Water

Water sampled at 5 cm was shown to be more enriched heavier isotopes, but as we sampled deeper, samples become more depleted (Figure 9). Soil water at the surface was enriched in both isotopes over the period, in addition, rainfall was prevalent during the period and conditions were changing on the surface weekly. The 5 cm samples were used to calculate the soil evaporation throughout the period, using additional variables for temperature and humidity conditions for each half hour period (Table 2).

5.1.2. Transpiration

After analyzing the stem samples through the Picarro instrument the samples from each day were averaged to obtain the isotopic composition of stem water (and transpiration at steady state) (Table 1). During the sampling period, we found that the composition of the stem water was significantly more enriched than that of the soil evaporation due to fractionation at the evaporative surface during evaporation. Stem water was shown to have enrichment over the 30-day period. This might suggest that the surface water was making it down to the roots. While the stem water delta values were taken at 1:00pm, the values are assumed to be valid throughout the entire period.

5.1.3. **Evapotranspiration**

We used Keeling plots to find the isotopic composition of total ET flux (Figures 10 and 11). We produced the Keeling plots by taking the last three minutes of data for each 5 min subsection and averaging those data points, then plotting the isotopic value over the inverse of specific humidity. For this reason, each Keeling plot represents a 30-minute period (Table 3). The Keeling plots for June 30th have been removed as the linear regression plots made no sense, linear values of 0 or explained variances of 0 with small confidence intervals, for the plots this is obviously not correct, a machine error was the most likely cause. While not all Keeling plots fall within the T and E end points, most of the Keeling plots do fall between these end points. The explained variance of the plots is low, and calls into question the validity of the Keeling plot analysis. The confidence intervals of the Keeling plots also show that few plots pass a 95 percent confidence test (Table 4).

5.1.4. **Statistics of the Keeling plots.**

The Keeling plots, as with any linear regression, are prone to have errors when the relationship of the variables is not linear. After taking T and E end point into account, we can see that the Keeling plots usually fall within those bounds. If the Keeling plot does not fall inside of those end points it is not used, as it will give us values for transpiration above 100 percent or below 0. For the analysis of June 30th and July 9th most of the Keeling plots

fail the 95% confidence test (Table 4). On the 16th of July however, almost all of the Keeling plots for the ^{18}O tracer passed the confidence test but the Deuterium Keeling plots did not fare as well. This will be discussed later after the results of the transpiration partitioning have been analyzed. Daily Averages, with and without drift correction

After obtaining the isotopic composition of ET using the Keeling plot method for all days during the period of analysis, the mid-day ET isotopic composition was averaged for each day, the following results show how the flux changed throughout the period of analysis (Figure 12). Please note that Figure 12 shows the results using raw data, without drift correction. There is no distinct pattern for the daily averages of Deuterium or ^{18}O (figure 12); we see that both tend to remain in a certain range of about -100 to -130‰ for δD and about -8 to – 16‰ for $\delta^{18}O$ but there is significant variability within that range. However, taking the normalized plots side by side (Figure 13 top) we can see a clear pattern. This pattern of concurring normalized values occurs from the 24th of June, until the 9th of July, it occurs again from the 19th of July, until the end of the sampling period on the 26th of July. After looking at synoptic scale events, it was found that prior to, and after the 10 day period in question, the winds at 700mb were from the west southwest or south for most of the days. During the 10 day period when the patterns tended to diverge, winds tended to be zonal or from the north-northwest. It

is also of some note that during the period in question no hurricane or tropical depressions were located in the Gulf of Mexico. Prior to, and following our anomaly, we saw a tropical storm or hurricane in the gulf that impacted Mexico or along the Texas border. During these periods of tropical activity there seemed to be a low level jet coming out of the Gulf of Mexico and running into New Mexico at 850mb. These events may be what cause the pattern to emerge. This shows a distinct link between synoptic scale events and the average Keeling plot charts. However, the objective of the Keeling plots is to isolate the ecosystem water vapor from external water vapor, and we shouldn't see the influence of synoptic-scale patterns from the data of the Keeling plots. After applying drift correction and plotting the new daily averages (Figure 13 bottom), the new data showed that with the drift correction, the day to day gradients varied similarly in $\delta^{18}O$ and δD, and presented no clear pattern developing over any period.

5.2. Transpiration Partitioning

5.2.1. Keeling Method

We performed the transpiration partitioning (Table 5) using the Keeling plots that fell within the T and E end points. Keeling plots appear to work best in the afternoon hours, but this is using only two days, as we only had afternoon data for June 27th and July 16th, with a larger number of days this could prove to be a statistical anomaly.

The Keeling plot transpiration values for each half-hour period were averaged, to give a single daily transpiration percentage (Table 6). For the 30th of June, we found that using the ^{18}O tracer showed that 70 percent of ET was from T but using the Deuterium tracer showed that 56 percent of evapotranspiration was from transpiration. For the 9th of July, in which we only have morning data due to rainfall, we find that about 80 percent of ET comes from transpiration using both ^{18}O and D. On the 16th of July, in which we only have data in the afternoon, we find that 55 percent of the ET was transpiration using ^{18}O as a tracer and that 15 percent of ET is from transpiration using Deuterium as our tracer.

5.2.2. **Multi-level Method**

The second method for calculating transpiration was our new multi-level method. In this method the absolute humidity and isotopic composition were averaged over the time periods and then the total daily transpiration was calculated. By averaging the values over the time period we eliminated some of the issues within the canopy due to small scale turbulence. The results of the multi-level method were similar to that of the Keeling plot method (Table 7). For the 30th of June, we found 79 percent of ET for the ^{18}O tracer and 84 percent for the Deuterium tracer, were from transpiration. For the 9th of July, we found that, of total ET, 69 percent and 79 percent were from transpiration using the ^{18}O tracer and Deuterium tracer respectively.

And we found that for the 16th of July, 58 percent of ET came from transpiration using the ^{18}O tracer while only 23 percent came from transpiration using the Deuterium tracer. Comparison of the multi-level method to the Keeling method

Both methods proved to have about the same percentages of transperation for each of the three days with slight differences. On the 30th of June, the multi-level method shows a higher transpiration, about 15 percent more than the Keeling plot method. The Deuterium tracer had a much larger difference than the ^{18}O tracer. For July 9th the percentages for transpiration were very close on the Deuterium tracer but had more variability with the ^{18}O tracer, all values for both methods fell close to each other. This suggests that for July 9th, we have a reasonable estimate of transpiration percentage for the times in question. On July 16th, the values for the ^{18}O tracer are reasonably close to each other as well as the Deuterium tracers. However, the two tracers show a different story on July 16th, with over a 30 percent difference in transpiration percentage between the two tracers.

6. DISCUSSION

6.1. Keeling plot analysis

The Keeling plot analysis is critically dependent on the large isotopic difference between transpiration and soil evaporation (Wang and Yakir, 2000), therefore transpiration fluxes are heavily dependent on the steady state assumption in the leaf stomata. However, the isotopic composition of the leaves does vary throughout the day (Harwood et al, 1999). An average of the Keeling plots throughout the day was taken to account for small changes in isotopic composition that were not measured. As seen in Table 5 transpiration percentage throughout the day can be variable and is dependent on many factors including temperature, relative humidity, and isotopic composition of the air outside the leaf. During steady state we can still see a small deviation from stem isotopic composition to transpiration of 1-3‰ for $\delta^{18}O$ (Flanagin et al., 1991, Wang and Yakir, 1995). In our analysis, this small percentage was most likely averaged out when taking the average of all the trees sampled.

The Keeling plots in our analysis had low explained variances and larger than expected confidence intervals, this calls into question the accuracy of the Keeling plot analysis. High winds throughout the area and large changes in sensible heat throughout the day suggest turbulence was present throughout

the measuring periods. Because the Keeling plots rely on stable conditions with little turbulence transport to make a highly accurate measurement, during times of high instability the Keeling plots will not perform well. Our results for the Keeling plots tend to fall in line with those that Yepez et al., 2003 found in a semi-arid woodland. The results of Yepez et al., 2003 show that in a semi arid Mesquite (Prosopis veluntina Wooton) dominated woodland with caespitose grass (Sporobolus wrightii Munro ex scribn) the total T flux was 88% when using ^{18}O as a tracer and was 85 % when using Deuterium as a tracer. Our results shown in Table 6, conclude that our semi arid woodland ET flux was slightly lower but within reason.

No water bodies were within a distance close enough to influence the ET flux in our study area and no evaporation from direct pooling on leaves or the soil was expected during any of the time periods monitored. However, on the 9th of July direct pooling could have been possible due to rainfall the prior two days although, no pools were actually observed. These conditions are critical to using the Keeling plot method. Additional sources of water vapor from an evaporating pool can critically change the results of the transpiration partitioning. Water sources besides the stomata and soil medium cannot be assumed as they will change with time and were not measured.

The end points play a crucial role in the partitioning of E and T. The measurement of these end points is highly critical to find the total E or T

fluxes. If the leaf is not at steady state the measurement of T will be wrong. The same can go for E, if the measurement is taken incorrectly or not all of the soil water is extracted in the cryogenic extraction process the isotopic composition of E will be incorrect. It has also been shown (RothFuss et al. 2010) that the depth of the soil sample is critical to finding the true isotopic composition of the E flux. Keeling plots that fall outside of the end points are of no use. We have numerous plots that fell outside the endpoints. This is to be expected and has happened in other experiments like ours. Moreira et al, 1997, shows that not all of the plots in their experiment fell within the end points.

6.2. Multi-level analysis

The new multi-level analysis proved to be effective over full day averages but due to the nature of the data, would not be suitable for half hour periods where turbulent mixing is occurring. This method relies on the assumption that the canopy is always more humid than the atmospheric boundary layer, while this assumption holds true for most situations, this will not always be the case. A few simple situations can occur, such as upper level moisture influx due to a low level jet or a highly turbulent day in which upper air is quickly mixing into the canopy making the two levels indistinguishable As with the Keeling plot method, open sources of water could contaminate the results if located close to the measurement inlets. The multi-level method

can also be influenced by dry sections within the canopy due to upper air mixing inside the canopy, as we used the assumption that the upper most level is representative of air outside the ecosystem. In many cases, it was found that the mid levels were actually drier then the top level, however, the bottom layer tended to be less affected due to zero plane displacement theory (less mixing due to low wind speed). This also tended to be the case in our upper levels, where canopy structure decreased mixing and by adding transpiration directly to these levels where leaves were abundant. Placing tubes higher above the canopy may also help with this measurement, as our tubes were around 10 to 12 meters above the canopy. This method may provide more useful information in a canopy where mixing is much less prevalent or where the layer beneath the foliage throughout the canopy is much more dense such as a rainforest or lowland hardwood forest.

6.3. Insights into instrumentation and improvements to sampling procedure.

6.3.1. Instruments

The Picarro instrument needs to be calibrated against a standard in order to ensure the isotopic values are accurate. Calibration of the specific humidity measurements is problematic, as shown with the NCAR LiCor data. Biases in the absolute humidity data can play a crucial role in the Keeling plots as higher humidity levels shift the plots to the right or left causing shifts in the

y-intercept. We believe the Licor data to be more within reason based on the weather instrumentation from other instruments at the site that are more in line with that data set even though their accuracy is not as precise. The y-intercept is the crucial factor in the Keeling plots, consequently, a shift left or right has an effect on the y-intercept value which in turn affects transpiration percentage. Depending on the slope of the Keeling plot, a bias in the humidity measurements can have no effect on the y-intercept or can change the y-intercept by a large percentage if there is a large slope, larger slopes having higher errors.

6.3.2. **Sampling Procedure**

The stem samples must be taken after the plants have achieved steady state transpiration, we assumed that the trees had achieved steady state at 1:30pm. The soil samples were collected at 1:00pm each afternoon at 6 different depths, while only the 5 cm depth was used, is has been shown that the depth of the soil sample has a large effect on the isotopic composition of the evaporation, sampling as close to the surface as possible tends to show the true isotopic composition of the evaporation flux (Rothfuss et al., 2010). Sampling throughout the day could also show a change in the surface conditions that could lead to changes in the calculated evaporation fluxes. This is especially true for days in which the soil medium was visibly dry, where the isotopic composition of the soil water could change throughout the

day. This could challenge the assumption that the soil water at the surface is a large enough to be considered an infinite source.

The sampling levels on the chemical tower in which the Picarro instrument was fitted to were already set and thus we had no control over them. In the future though using a higher top level could be used for the atmospheric conditions used in the multi-level approach. The better the measurement of the ambient air is, before ET flux is mixed in, the better the results should be.

7. CONCLUSION

Our study resulted in the partitioning of transpiration in a semi-arid forest. We performed a statistical analysis of the data set and discovered ways to improve the data set to account for atmospheric structure and time drift in the dataset. The results of the Keeling plot method and the multi-level method introduced show similar results and this shows the multi-level method could be promising in the future.

The results of this study show some theoretical downfalls with the Keeling plot analysis. While the Keeling plot may work well in stable environments we can see from the results, that it does not fare well during periods of intense atmospheric mixing. The multi-level method can address some of the issues with the Keeling plot method and when compared to the Keeling plot method performed well. Of course this assumes we believe the results the Keeling plots provide. The multi-level method is shown to be more robust when measuring isotopic levels using a high frequency technique.

APPENDIX A TABLE AND FIGURES

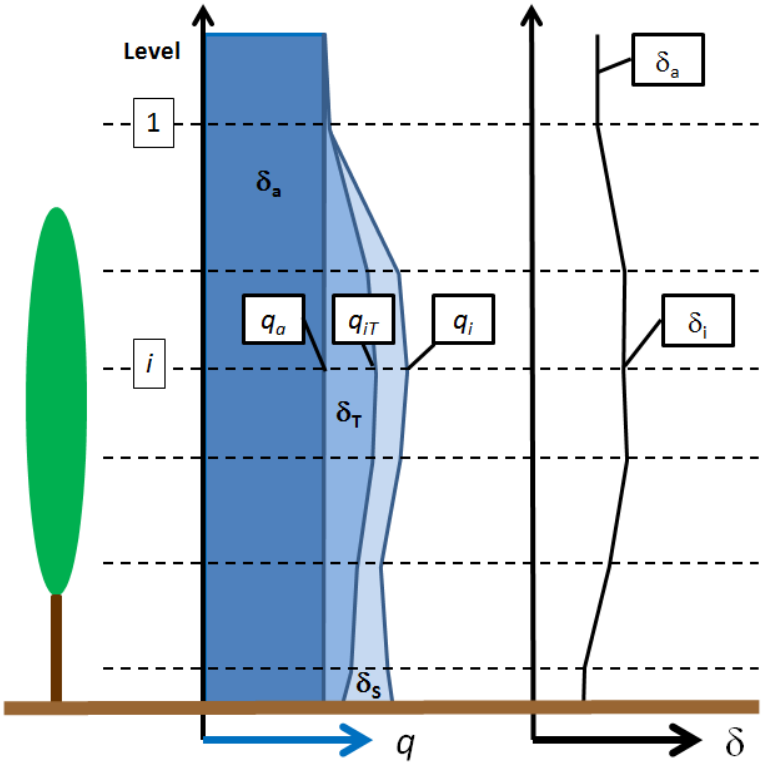

Figure 1 shows a diagram of how the multi-level method will work. The green oval represents the foliage of the area. δ_a δ_T δ_s represent the isotopic composition of the atmosphere, transpiration, and soil evaporation respectively and q_a q_{iT} and q_i represent the specific humidity of the atmosphere transpiration and soil evaporation respectively. δ_i represents a mixing of the three. This graphic is just an illustration and does not represent what all plot would look like but the basic idea behind the multi-level method.

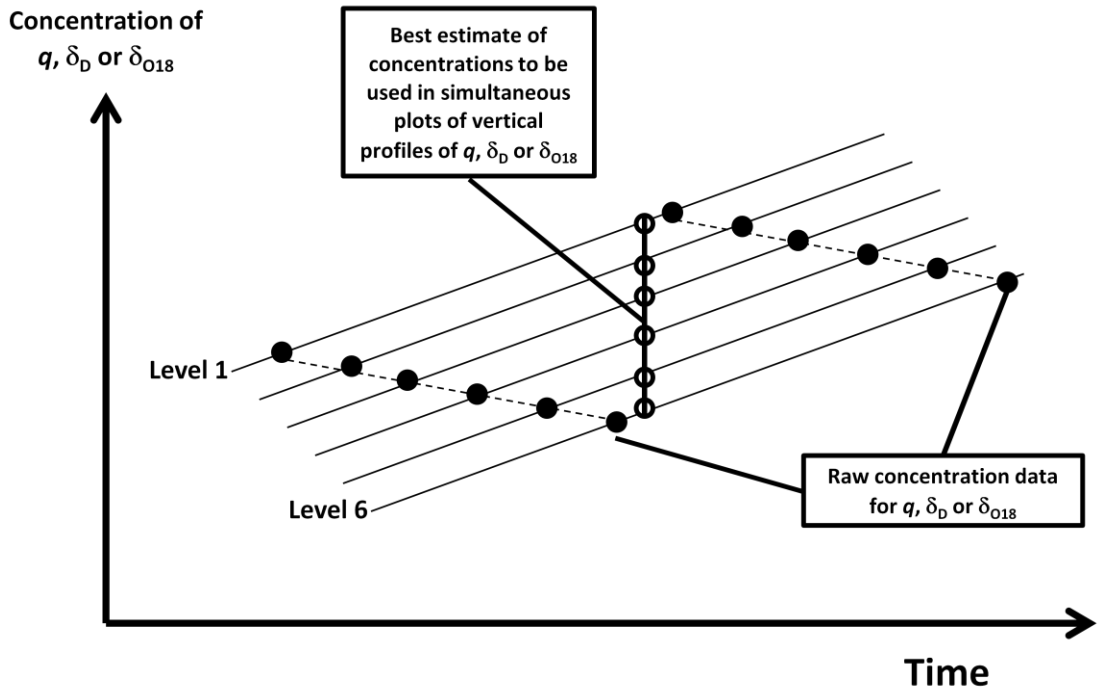

Figure 2 Shows the theory behind the drift correction we applied. The black circles represent actual data. The open circles represent what the corrected date would look like.

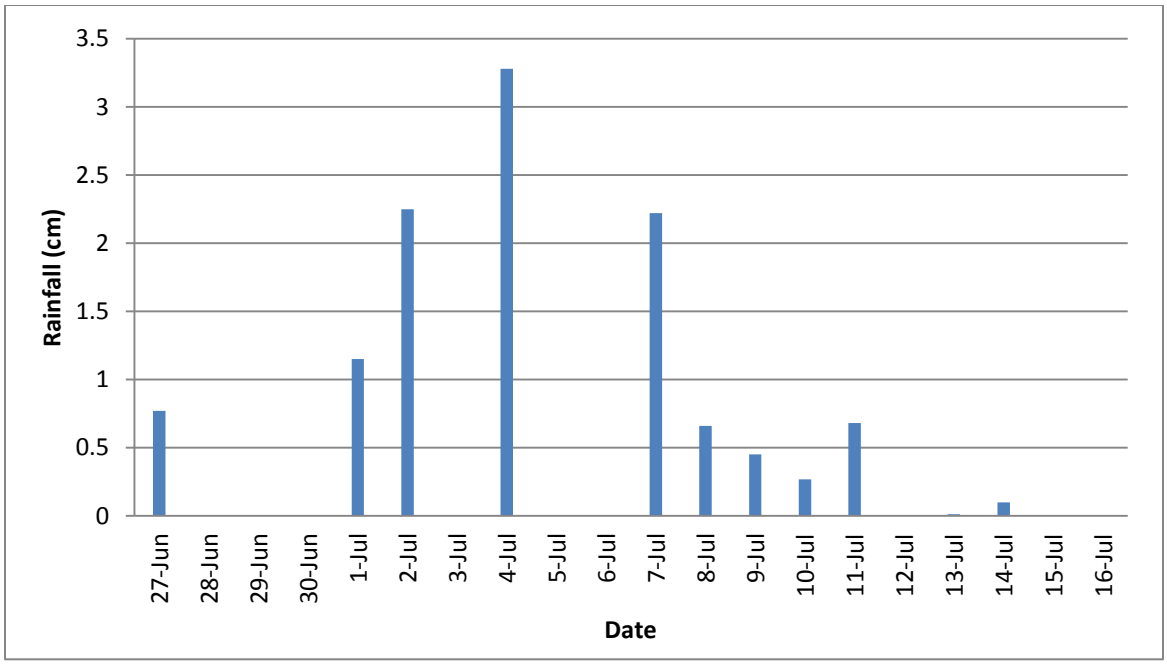

Figure 3 Rainfall throughout the measurement period in 2010.

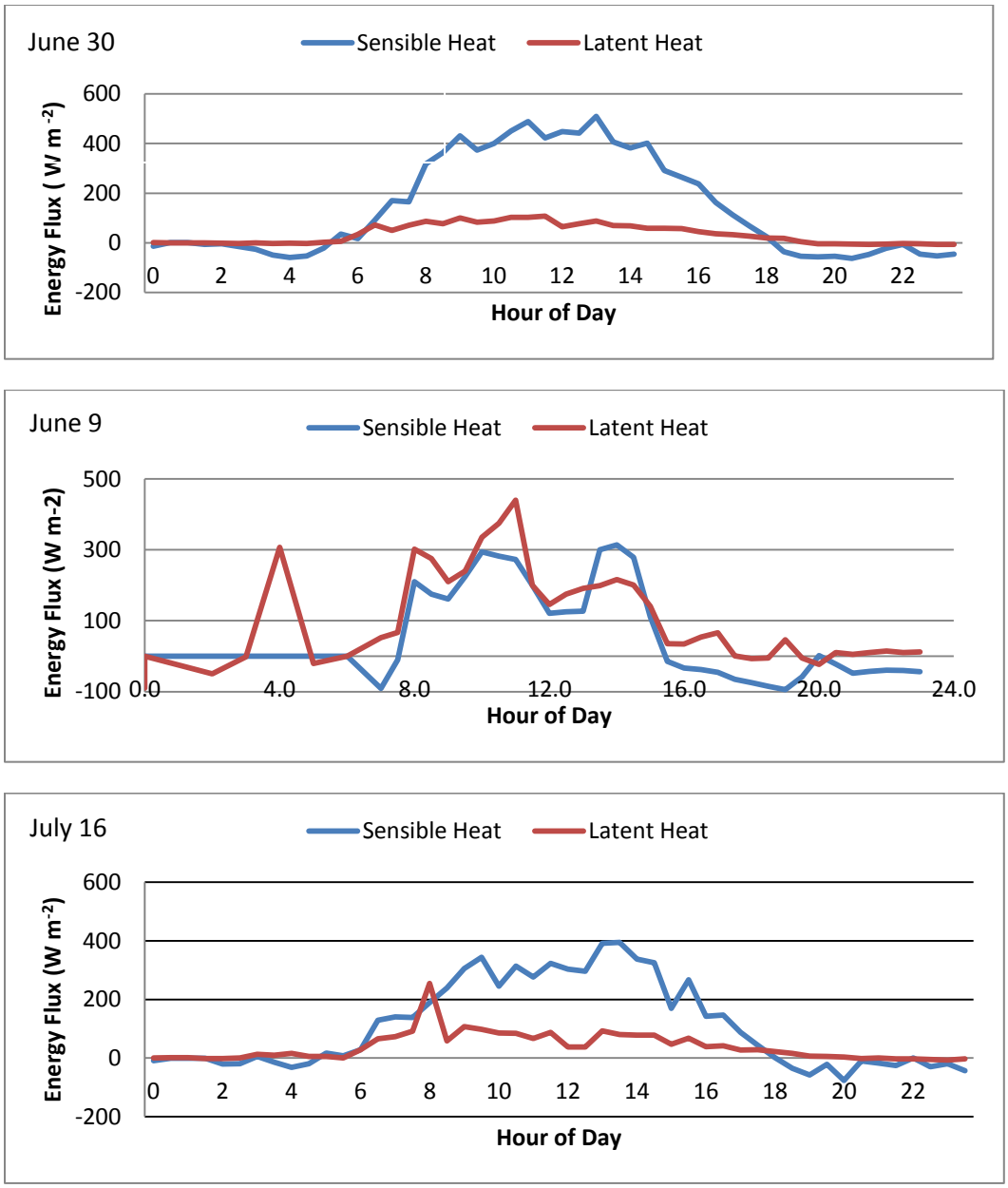

Figure 4 Sensible and latent heat profiles throughout the three days. June 30th (top) shows the sensible heat is dominating where energy is going to as the soil conditions were dry due to lack of rainfall in the prior two days. July 9th (middle) shows that latent heat and sensible heat are almost equal at taking up energy throughout the day this is most likely caused by a wet soil medium from the two previous day's rainfall events. July 16th (bottom) shows that again sensible heat is the dominant source of energy uptake.

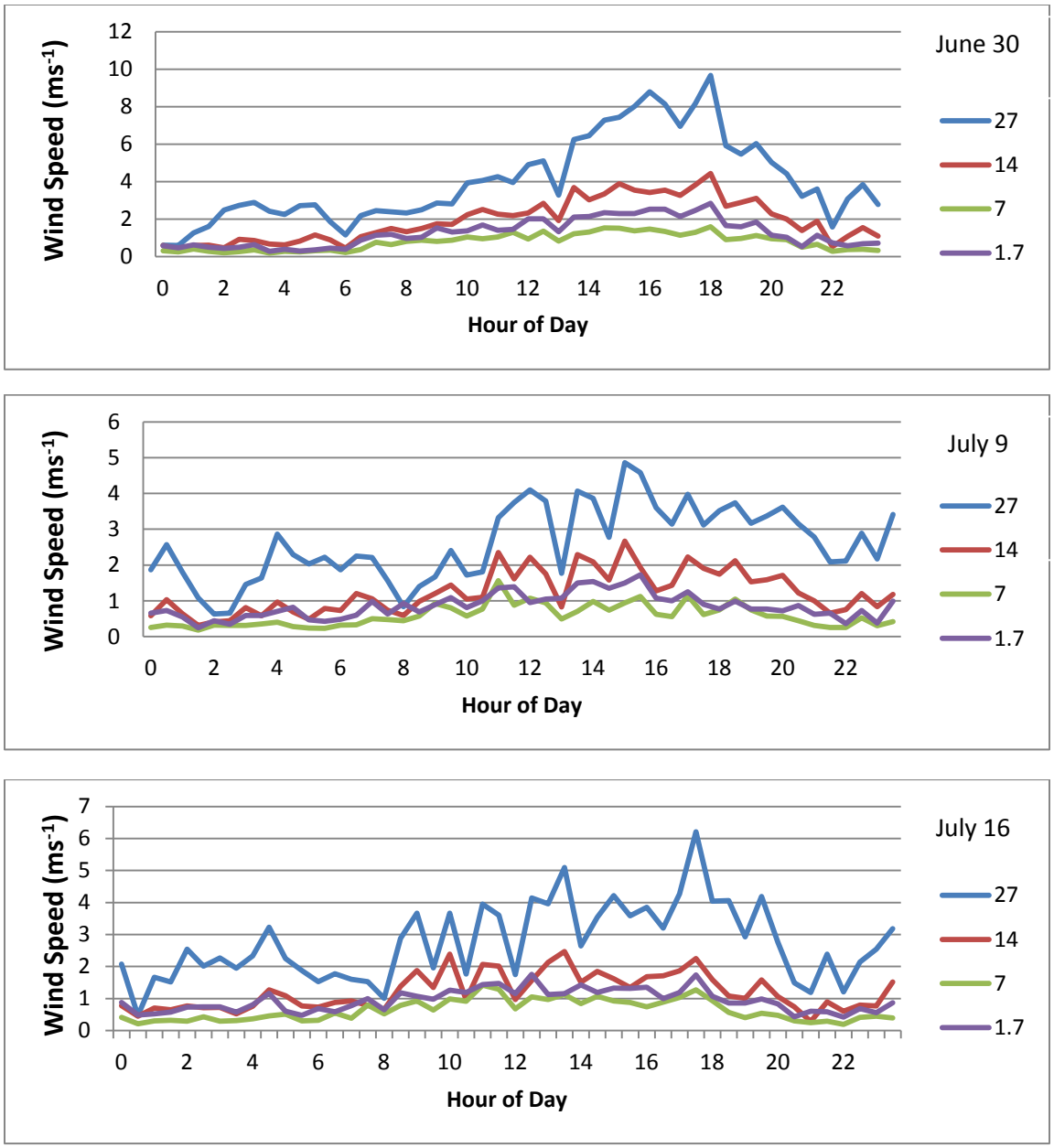

Figure 5 Shows the wind speeds over the three days in which transpiration percentage was calculated. The figures top to bottom are June 30th July 9th and July 16th with the plots from all four levels in meters.

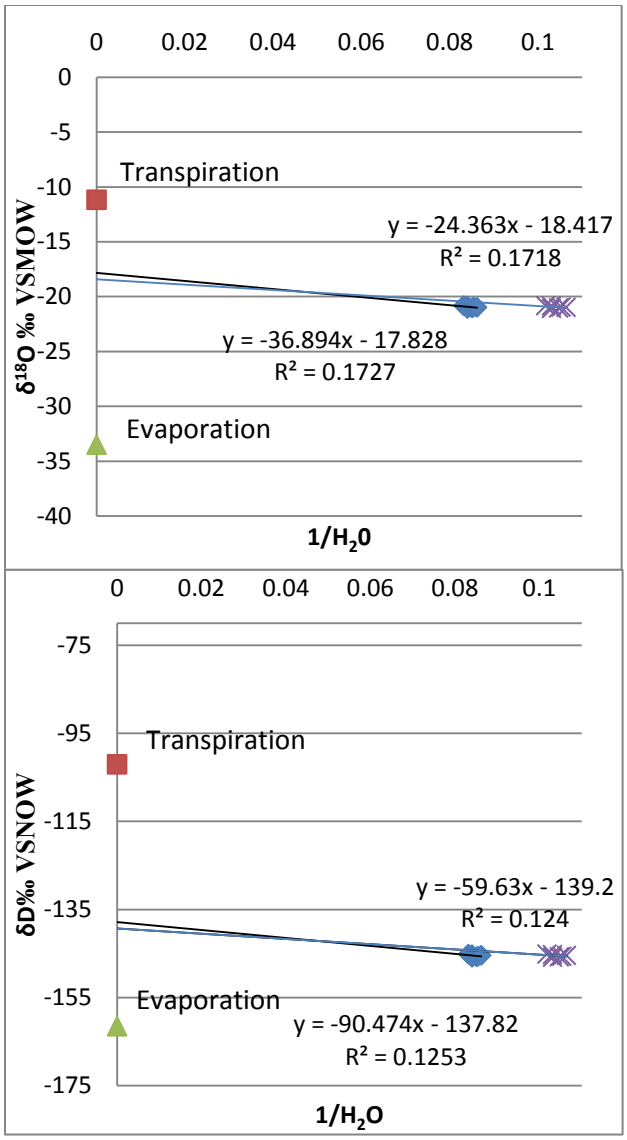

Figure 6 Shows drift corrected Keeling plots with specific humidity corrected and raw data for July 16th at 3:30 pm. You can see the blue line and X's which is shift correct to the NCAR data, is almost identical to the non-shift corrected raw data from the Picarro instrument.

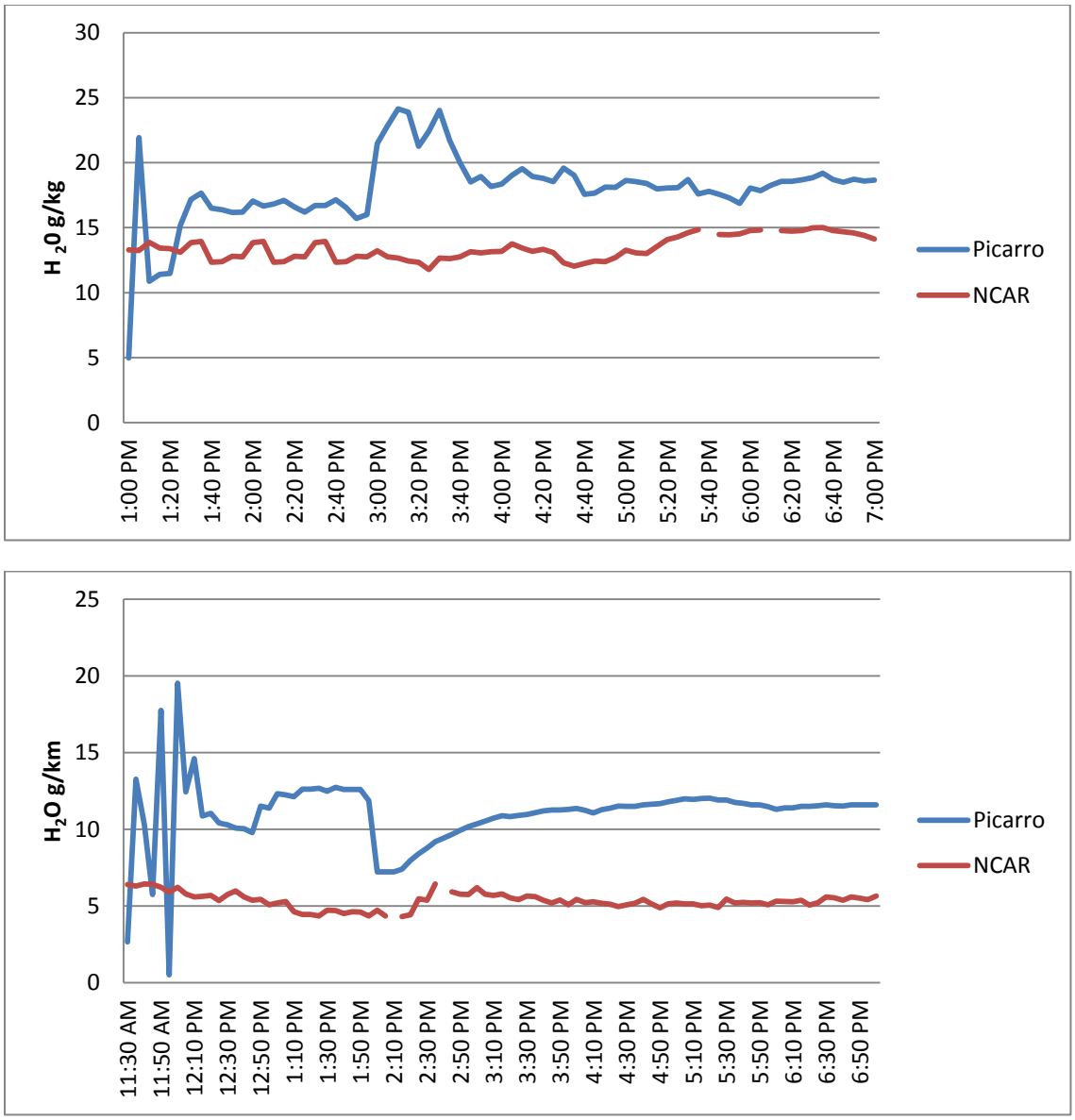

Figure 7 Shows (top) July 9th and (bottom) July 16th absolute humidity values measured by each instrument throughout the day. No NCAR data was available on the 30th of June.

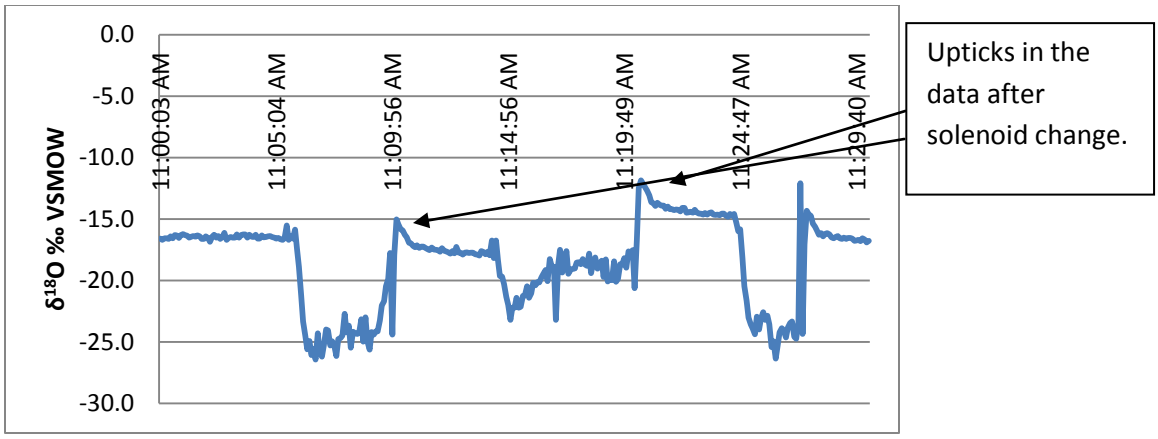

Figure 8 Shows a typical $\delta^{18}O$ half hour period through the dataset. This is July 9th at 11:30am; you can see the changed in the solenoid valve opening clearly on the graph. This is the reason for the first two minutes of data being thrown out for the averaging.

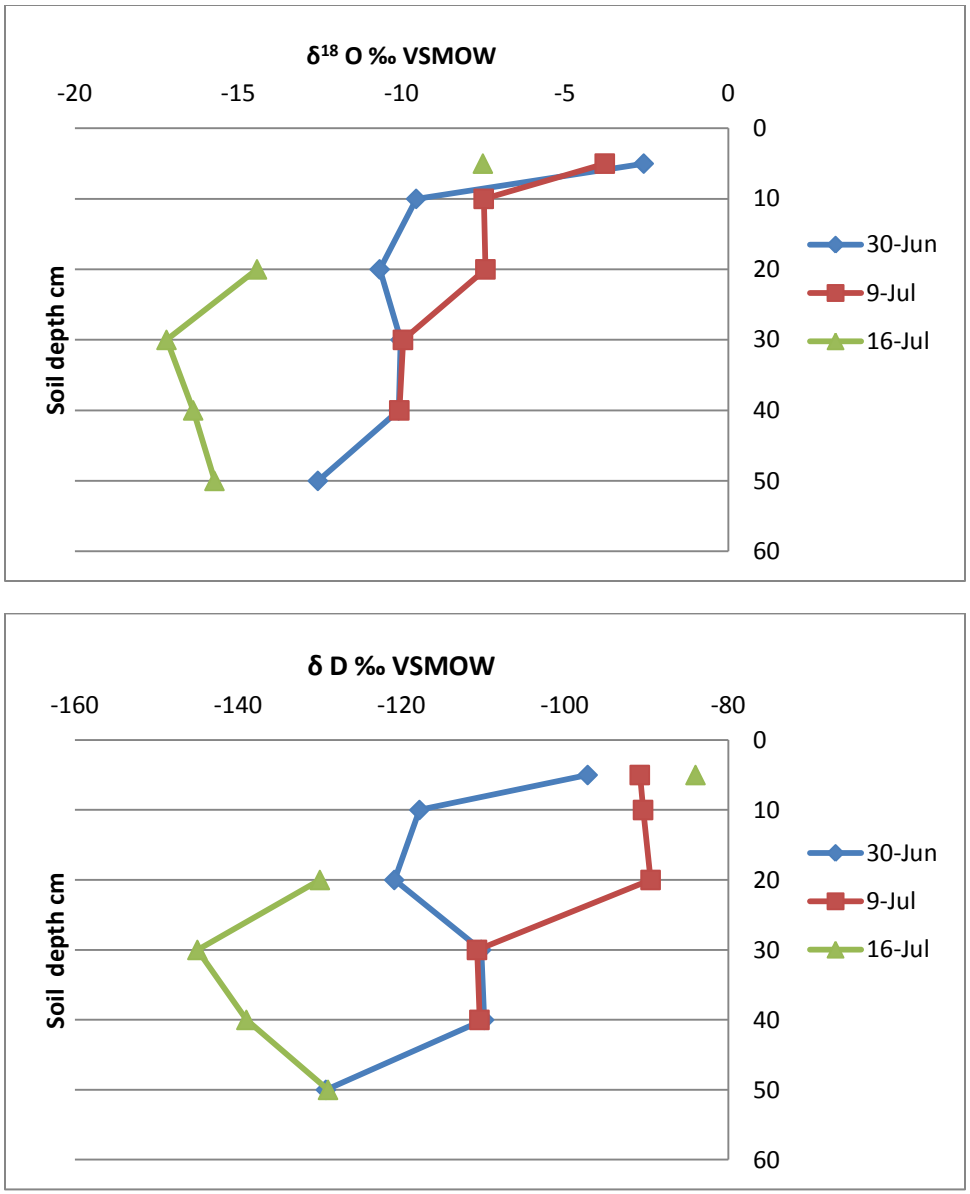

Figure 9 Shows the isotopic value of the soil samples with respect to sampling depth.

30-Jun	$\delta^{18}O$ Evap‰	δD Evap ‰	9-Jul	$\delta^{18}O$ Evap‰	δD Evap‰	16-Jul	$\delta^{18}O$ Evap‰	δD Evap‰
8:00	-26.15	-179.45	8:00	-27.78	-182.85	8:00	-32.88	-166.31
8:30	-27.93	-177.42	8:30	-28.75	-181.66	8:30	-33.36	-163.06
9:00	-27.79	-176.74	9:00	-29.26	-179.20	9:00	-33.72	-161.44
9:30	-27.82	-176.01	9:30	-29.94	-178.94	9:30	-33.84	-161.86
10:00	-28.15	-175.61	10:00	-29.74	-179.23	10:00	-34.44	-160.90
10:30	-28.23	-175.19	10:30	-28.52	-178.50	10:30	-34.39	-160.52
11:00	-28.39	-175.03	11:00	-28.41	-181.34	11:00	-34.39	-159.89
11:30	-27.83	-174.87	11:30	-28.28	-186.05	11:30	-34.35	-159.52
12:00	-27.95	-174.75		Rain	Rain	12:00	-34.34	-159.22
12:30	-27.86	-175.24				12:30	-34.34	-158.98
13:00	-27.92	-175.24				13:00	-34.24	-158.78
13:30	-28.06	-175.02				13:30	-34.26	-158.26
14:00	-27.96	-175.56				14:00	-34.25	-158.20
14:30	-27.96	-175.77				14:30	-34.23	-157.93
15:00	-27.86	-175.97				15:00	-34.32	-158.89
15:30	-27.82	-176.89				15:30	-34.35	-159.36
16:00	-28.00	-177.49				16:00	-34.34	-159.35

Table 1 Shows the half hourly isotopic composition of evaporation from the soil medium using equation 13. It rained at 12:00pm on the 9th thus soil samples may no longer be representative of what the isotopic composition of the soil is and thus those numbers have been excluded from the table.

Date	30-Jun	9-Jul	16-Jul
stem $\delta^{18}O$‰	-14.8228	-13.7135	-11.1688
stem δD‰	-126.752	-116.175	-102.02

Table 2 Shows the isotopic composition of the stem water on June 30th July 9th July 16th .

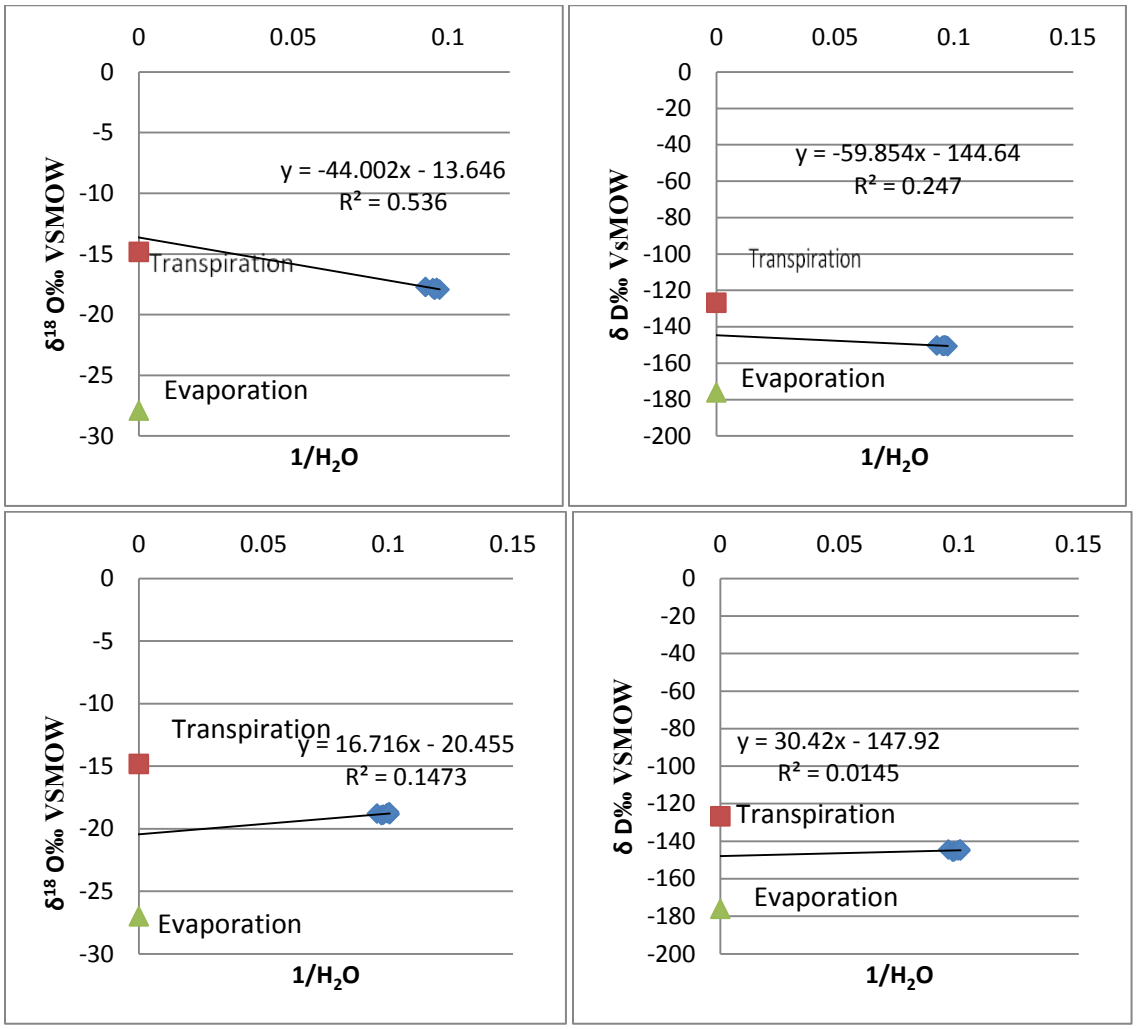

Figure 10 Shows the Keeling plots for June 30th at 8:30am top and 11:00am bottom for both $\delta^{18}O$ and δD. The plots show the transpiration and soil evaporation bounds as well as the equation for the linear regression with the explained variance. On the 8:30am plot for $\delta\ ^{18}O$ we can see that the y-intercept does not fall within the transpiration and soil evaporation end points.

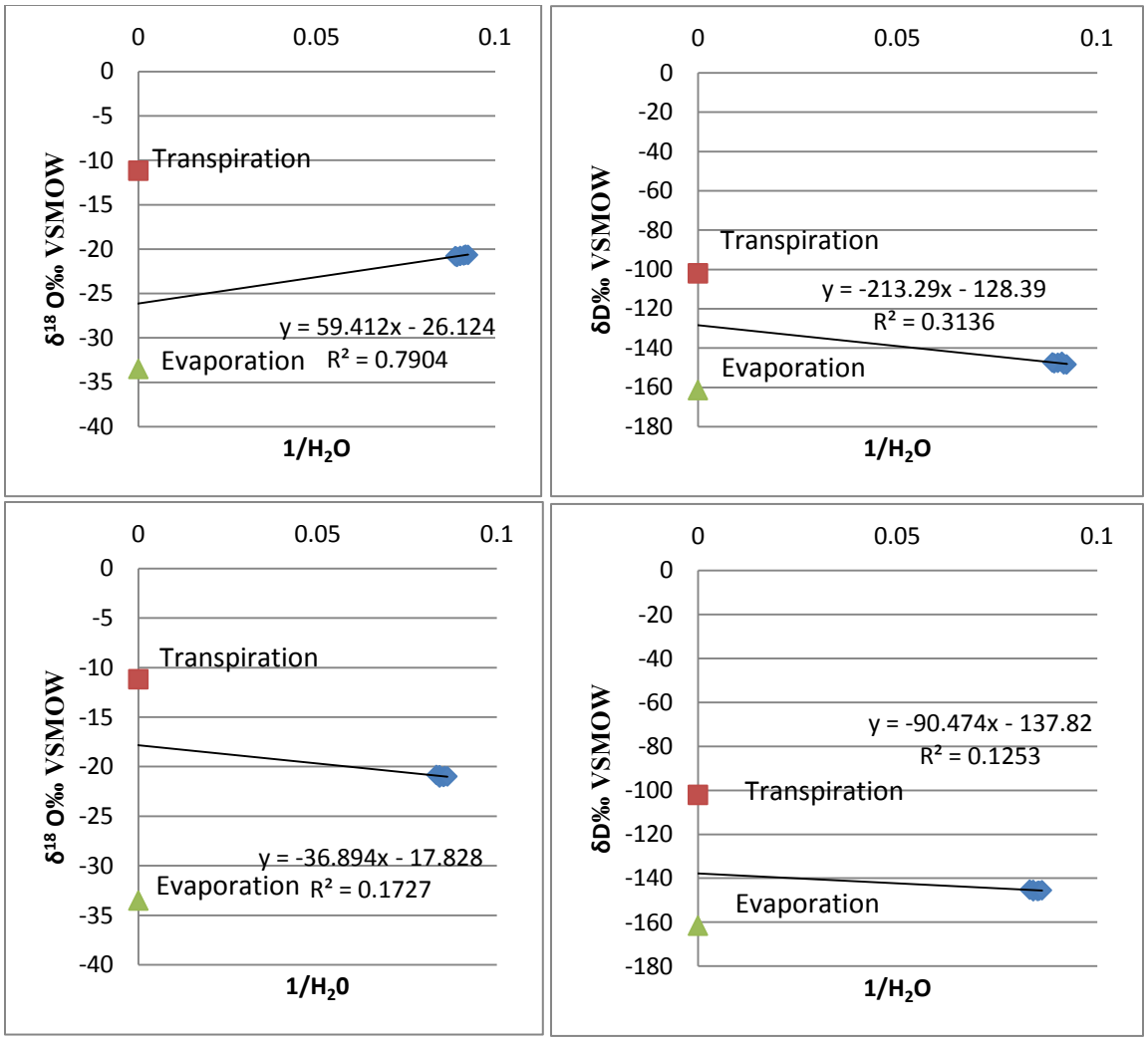

Figure 11 Shows the Keeling plots for July 16th at 1:30pm top and 3:30pm bottom. The plots show the linear regression and explained variance along with the transpiration and soil evaporation bounds.

30-Jun	Y intercept $\delta^{18}O$	+/-	R^2	Y intercept δD	+/-	R^2
8:30	-20.01	8.75	0.01	-165.99	50.41	0.03
9:00	-20.03	12.10	0.00	-161.93	74.60	0.02
9:30	-20.46	5.51	0.15	-147.92	34.32	0.01
10:00	-13.79	6.86	0.49	-118.85	48.51	0.33
10:30	-17.32	15.07	0.01	-141.74	94.40	0.00
11:00	-17.20	1.58	0.60	-136.48	9.29	0.41
13:30	-15.62	8.21	0.20	-131.93	42.97	0.10
14:00	-14.69	7.28	0.34	-118.22	50.68	0.30
14:30	-22.58	6.98	0.41	-164.12	38.16	0.39
15:00	-16.46	1.84	0.78	-136.24	7.25	0.76
15:30	-18.25	0.70	0.87	-143.44	5.95	0.66
16:00	-14.60	4.47	0.71	-125.76	30.68	0.55

9-Jul	Y intercept $\delta^{18}O$	+/-	R^2	Y intercept δD	+/-	R^2
8:00	-6.33	20.79	0.22	-42.80	158.22	0.23
8:30	-10.23	12.93	0.24	-76.88	117.24	0.15
9:00	-16.29	1.69	0.20	-121.30	14.59	0.20
9:30	-15.38	1.17	0.75	-90.60	21.98	0.83
10:00	-46.12	147.90	0.07	-110.12	874.33	0.00
10:30	-16.19	2.43	0.62	-122.73	23.58	0.27
11:00	-64.96	68.64	0.50	-67.64	160.34	0.20
11:30	-17.23	6.50	0.05	-134.93	16.32	0.00

16-Jul	Y intercept $\delta^{18}O$	+/-	R^2	Y intercept δD	+/-	R^2
12:00	-20.95	10.70	0.16	-151.57	55.04	0.39
12:30	-23.79	11.72	0.03	-183.41	102.74	0.01
13:00	-15.72	16.88	0.34	-43.41	297.85	0.28
13:30	-23.59	1.41	0.59	-150.43	19.92	0.18
14:00	-21.24	0.79	0.08	-153.43	3.38	0.58
14:30	-19.90	1.37	0.38	-146.45	4.82	0.23

15:00	-22.32	6.77	0.09	-152.05	30.84	0.04
15:30	-19.34	2.26	0.47	-136.91	11.00	0.60
16:00	-22.63	2.78	0.45	-149.48	11.99	0.17

Table 1 Shows the y-intercept values with confidence intervals and explained variance for all keeling plots produced.

Date	Total Plots	$\delta^{18}O$ within ET	$\delta^{18}O$ within Confidence	δD within ET	δD within Confidence
30-Jun	12	7	3	7	3
9-Jul	8	6	3	4	1
16-Jul	9	9	4	8	3

Table 2 Shows the total amount of Keeling plots for each tracer and if the plot fell within the transpiration and soil evaporation bounds. The confidence intervals were also evaluated and if the y-intercept confidence interval fell within the bounds as well. The ^{18}O tracer seems to have better results than the Deuterium tracer.

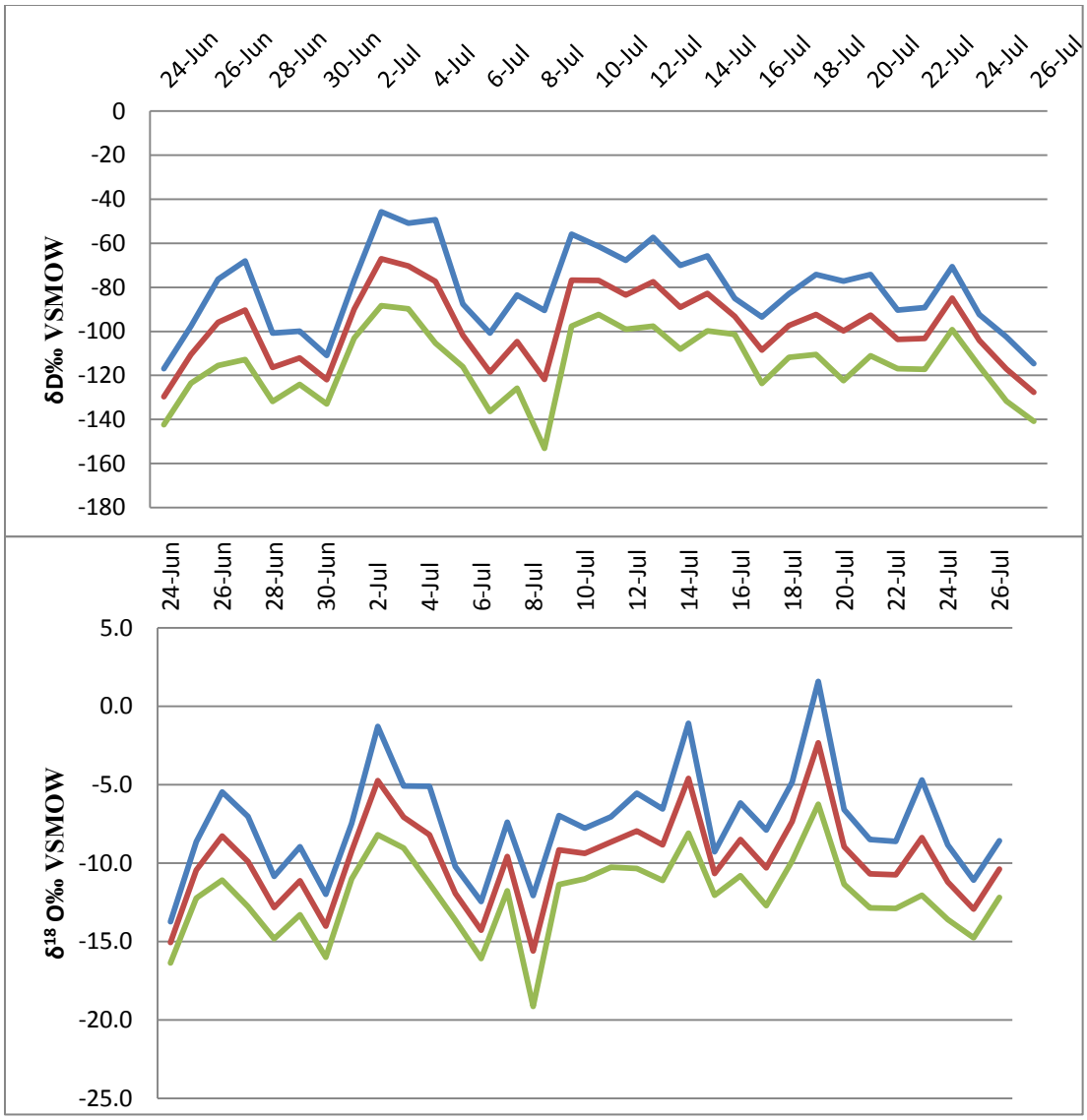

Figure 12 Daily Variability of δD (top) and $\delta^{18}O$ (bottom) for all the days of analysis. Blue line is upper bound confidence interval and the green line is the lower bound confidence interval.

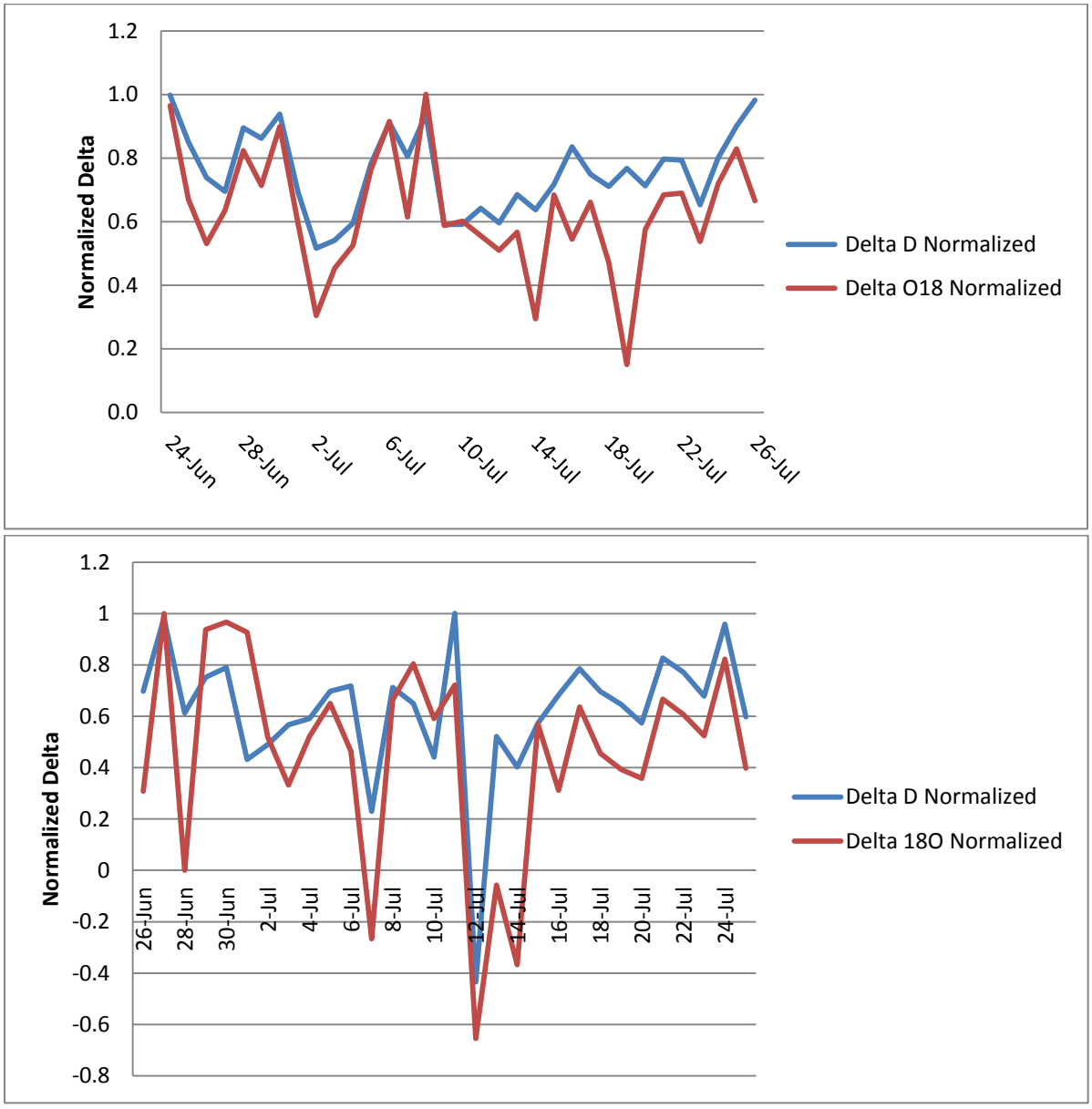

Figure 13 (Top)δD and $\delta^{18}O$ normalized showing the daily changes as you can see at July 9th a change occurs in the pattern that reemerges at July 19th. (Bottom) δD and $\delta^{18}O$ normalized after drift correction has been made. The pattern that had emerged without drift correction is now gone.

	30-Jun		9-Jul		16-Jul	
	δD Ft	δ ^{18}O Ft	δD Ft	δ^{18}OFt	δD Ft	δ^{18}O Ft
8:00	No Data	No Data	93.30	79.18	Machine	Malfunction
8:30	27.33	60.42	~~133.45~~	87.54		
9:00	32.96	59.850	~~108.0~~	~~-139.83~~		
9:30	~~819.16~~	~~386.09~~	90.42	82.36		
10:00	~~234.27~~	~~155.58~~	~~172.34~~	~~-240.72~~		
10:30	~~348.34~~	~~210.52~~	71.17	77.35		
11:00	79.80	82.75	~~116.19~~	84.14		
11:30	NA	NA	70.82	73.23		
12:00	NA	NA	Rain	Rain	~~203.55~~	80.34
12:30	NA	NA			13.45	46.10
13:00	NA	NA			7.31	56.21
13:30	87.84	93.91			20.92	62.17
14:00	~~115.79~~	~~100.97~~			11.05	51.71
14:30	22.58	40.94			37.94	64.59
15:00	79.11	87.28			15.14	50.27
15:30	64.80	73.65			14.87	46.53
16:00	~~100.47~~	~~101.66~~			4.07	41.02

Table 3 Shows the Keeling plot transpiration values for each day using the two different isotope tracers. On July 9th rainfall occurred around 12:00 PM so all data after this could not be compared against the soil sample taken at 9:00 AM. On July 16th the Picarro Machine was malfunction in the morning and after a power outage reset itself for the afternoon. All number with lines through them were not used in the daily average transpiration calculation.

.

	Ft ^{18}O			
Keeling	%	Ft D %	Start	End
30-Jun	70.2	56.5	8:30	16:00
9-Jul	80.6	81.4	8:00	11:30
16-Jul	55.4	15.6	12:00	16:00

Table 4 Shows the average transpiration for the period using the Keeling plot approach. Values during the period that were above 100 % or below 0 were not included in the averaging.

Multi-Level	FT ^{18}O %	Ft D %	Start	End
30-Jun	79.6	84.5	8:30	16:00
9-Jul	69.9	79.9	8:00	11:30
16-Jul	58.1	23.7	12:00	16:00

Table 5 Shows the transpiration percentages calculated using the multi-level method.

REFERENCES

Baldocchi, D.D., Hicks, B.B., Meyer, T.P., 1988. Measuring biosphere-atmosphere exchanges of biologically related gases with micrometeorological methods. Ecology 69, 1331–1340.

Bosilovich, and S.D. Schubert, 2002: Water vapor tracers as diagnostics of theregional hydrologic cycle. *J. Hydrometeor.,* **3,** 149–165.

Bosilovich, and J. Chern, 2006: Simulation of water sources and precipitationrecycling for the MacKenzie, Mississippi, and Amazon River basins. *J. Hydrometeor.,* **7,** 312–329.

Brunel, J.P., Simpson, H.J., Herczef, A.L., Whitehead, R., Walker, G.R., 1992. Stable isotope composition of water vapor as an indicator of transpiration fluxes from rice crops. *Water Resource*. Res. 28, 1407–1416.

Craig, H., Gordon, L.I., 1965. Deuterium and oxygen-18 variations in the ocean and the marine atmosphere. In: Tongiori, E. (Ed.), Proceedings of the Conference on Stable Isotopes in Oceanographic Studies and Paleotemperatures. Laboratory of Geology and Nuclear Science, Pisa, pp. 9–130.

Dirmeyer, P. A., and K. L. Brubaker, 1999: Contrasting evaporativemoisture sources during the drought of 1988 and theflood of 1993. *J. Geophys. Res.,* **104,** 19 383–19 397.

Dominguez, F., P. Kumar, X. Liang, and M. Ting, 2006: Impact of atmospheric moisture storage on precipitation recycling. *J.Climate,* **19,** 1513–1530.

Dominguez, F., and P. Kumar (2008), Precipitation recycling variabilityand ecoclimatological stability—A study using NARR data. Part I: CentralU. S. plains ecoregion, *J. Climate.*, *21*(20), 5165–5186,

Dunin, F.X., 1991. Extrapolation of 'point' measurements ofevaporation: some issues of scale. Vegetation 91, 3947.

Ehleringer, J.R., Field, C., 1993. Scaling Physiological Processes: Leaf to Globe (Physiological Ecology). Academic Press, San Diego, 388 pp.

Ehleringer, J.R., Roden, J., Dawson, T.E., 2000. Assessing ecosystem-level water relations trough stable isotope ratio analysis. In: Sala, O.E., Jackson, R.B., Mooney, H.A., Howarth, R.W. (Eds.), Methods in Ecosystem Science. Springer, Berlin, p. 407.

Entekhabi, D., Asrar, G. R., Betts, A. K., Beven, K. J., Bras, R. L., Duffy, C. J., et al. (1999). An agenda for land surface hydrology research and a call for the second international hydrological decade. *Bulletin of the American Meteorological Society*, 80, 2043−2058.

Fisher, J. B., K. P. Tu, and D. D. Baldocchi, 2008: Global estimates of the land–atmosphere water flux based on monthlyAVHRRand ISLSCP-II data, validated at 16 FLUXNET sites. Remote Sens. Environ., 112, 901–919.

Flanagan LB, Ehleringer JR. 1991. Stable isotope composition of stem and leaf water: applications to the study of plant water use. *Functiona lEcology* **5**: 270–277.

Gat, J.R., 1996. Oxygen and hydrogen isotopes in the hydrological cycle. Annu. Rev. Earth Planet. Sci. 24, 255–262.

Jackson, R.B., Anderson, L.J., Pockman W.T., 2000. Measuring water availability and uptake in ecosystem studies. In: Sala, O.E., Jackson, R.B., Mooney, H.A., Howarth, R.W. (Eds.), *Methods in Ecosystem Science.* Springer, New York, 407 pp.

Jarvis, P.G., 1995. Scaling processes and problems. *Plant Cell Environ*. 18, 1079–1089.

Kalnay, E., Kanamitsu, M., Kistler, R., et al., 1996. The NCEP/NCAR 40-year reanalysis
project. *Bulletin of the American Meteorological Society* 77, 437–471.

Keeling CD. 1961. The concentration and isotopic abundances of carbon dioxide in rural and marine air. *Geochimica et Cosmochimica Acta* **24**: 277–298.

Mesinger, F., and Coauthors, 2006: North American Regional Reanalysis. *Bulletin of the American Meteorological Society*., **87,** 343–360.

Moncrieff, J.B., Jarvis, P.G., Valentini, R., 2000. Canopy fluxes. In: Sala, O.E., Jackson, R.B., Mooney, H.A., Howarth, R.W. (Eds.), *Methods in Ecosystem Science*. Springer, New York, 407 pp.

M.Z. Moreira, L.A. Martinelli, R.L. Victoria, E.M. Barbosa, L.C.M. Bonates and D.C. Nepstads, Contribution of transpiration to forest ambient vapour based on isotopic measurements. *Global Change Biol.***3** (1997), pp. 439–450.

Paruelo, J.M., Sala, O., 1995. Water losses in the Patagonian steppe: a modeling approach. Ecology 76, 510–520.

Pearcy, R.W., Ehleringer, J.R., Mooney, H.A., Rundel, P.W., 1989. Plant Physiological Ecology Field Methods and Instrumentation. Chapman & Hall, London, 457 pp.

Reynolds, J.F., Kemp, P.R., Tenhunen, J.D., 2000. Effects of long-term variability on evapotranspiration and soil water distribution in the Chihuahuan Desert: a modeling analysis. *Plant Ecol.* 150, 145–159.

Rothfuss, Y., Biron, P., Braud, I., Canale, L., Durand, J.-L., Gaudet, J.-P., Richard, P., Vauclin, M. and Bariac, T. (2010), Partitioning evapotranspiration fluxes into soil evaporation and plant transpiration using water stable isotopes under controlled conditions. *Hydrological Processes*., 24: 3177–3194.

Ruiz-Barradas, Alfredo, Sumant Nigam, 2006: Great Plains Hydroclimate Variability: The View from North American Regional Reanalysis. *J. Climate*, 19, 3004–3010

Salati, E.*, and* P. B.Vose. 1984. Amazon basin—a system in equilibrium. *Science* 225*:* 129–138.

Scott R, Entekhabi D, Koster R, Suarez M (1997) Timescales of land surface evapotranspiration response. *J. Climate* 10:559–566.

Scott, R., R. Koster, D. Entekhabi, and M. Suarez, 1995: Effect of a canopy interception reservoir on hydrological persistence in a general circulation model. *J. Climate,***8,** 1917–1922.

Shuttleworth, W., J. Gash, C. Lloyd, D. McNeill, C. Moore, and J. Wallace (1988), An integrated micrometeorological system for evaporation measurement, *Agricultural and Forest Meteorology*., 43(3–4), 295–317.

United States Department of Agriculture. Web. March, 2011.<http://www.fs.usda.gov/main/manitou/about/site-description>

Wang XF, Yakir D. 2000. Using stable isotopes in evapotranspiration studies. *Hydrological Processes* 14: 1407–1421.

"Simple Linear Regression Anaylsis." Web. Nov. 2011. <http://www.weibull.com/DOEWeb/simple_linear_regression_analysis.htm>.

Williams DG, Cable W, Hultine K, Hoedjes JCB, Yepez EA, Simmoneaux V, Er-Raki S, Boulet G, de Bruin HAR, Cheehbouni A, Hartogensis OK, Timouk F. 2004. Evapotranspiration components determined by sable isotope, sap flow and eddy covariance techniques. *Agricultural and Forest Meteorology* **125**: 241–258.

Yakir, D., Wang, X.F., 1996. Fluxes of CO2 and water between terrestrial vegetation and the atmosphere estimated from isotope measurements. *Nature* 380, 515–517.

Yepez EA, Williams DG, Scott RL, Lin G. 2003. Partitioning overstory and understory evapotranspiration in a semiarid savanna woodland from the isotopic composition of water vapour. *Agricultural and Forest Meteorology* **119**: 53–68.

Yepez EA, Huxman TE, Ignace DD, English NB, Weltzin JF, Castellanos AE, Williams DG. 2005. Dynamics of transpiration and evaporation following a moisture pulse in semirarid grassland: a chamber-based isotope methods for partitioning flux components. *Agricultural and Forest Meteorology* **132**: 359–376.